

# Novel edible films of pectins extracted from low-grade fruits and stalk wastes of sun-dried figs: Effects of pectin composition and molecular properties on film characteristics

Elif Çavdaroğlu<sup>a</sup>, Duygu Büyüktaş<sup>a,b</sup>, Stefano Farris<sup>b</sup>, Ahmet Yemenicioğlu<sup>a,\*</sup>

<sup>a</sup> Department of Food Engineering, Faculty of Engineering, Izmir Institute of Technology, 35430, Gölbaşı Köyü, Urla, Izmir, Turkey

<sup>b</sup> DeFENS, Department of Food, Environmental and Nutritional Sciences, Packaging Division – University of Milan, Via Celoria 2, 20133, Milan, Italy

## ARTICLE INFO

### Keywords:

Fig pectin  
Citrus pectin  
Edible film  
Cross-linking  
Barrier properties  
Mechanical properties

## ABSTRACT

This study aimed to explore the characteristics of novel fig pectin films. For this purpose, films of crude fig pectin (CFP) extracted from low-grade sun-dried fruits and films of crude (CSP) and purified (PSP) stalk pectins extracted from stalk waste of processed high-quality sun-dried figs were evaluated for their physicochemical properties. The properties of pristine (CFP, CSP, and PSP films) and CaCl<sub>2</sub> cross-linked films (CFP-Ca<sup>++</sup>, CSP-Ca<sup>++</sup> and PSP-Ca<sup>++</sup> films) of fig pectins were also compared with films of commercial citrus (CP and CP-Ca<sup>++</sup>) and apple (AP, AP-Ca<sup>++</sup>) pectins. The cross-linking improved the mechanical strength and barrier properties of most films. CP, CP-Ca<sup>++</sup>, PSP, and PSP-Ca<sup>++</sup> films showed greater mechanical strength and stiffness than other films. PSP-Ca<sup>++</sup>, PSP and CP-Ca<sup>++</sup> films showed the lowest water vapor permeability (6.28, 12.85, 14.96 g.mm.m<sup>-2</sup>.day<sup>-1</sup>.kPa<sup>-1</sup>, respectively) while CSP-Ca<sup>++</sup>, CP-Ca<sup>++</sup>, CP, PSP-Ca<sup>++</sup> films showed the lowest oxygen permeability coefficients (5403, 8265, 10776, 11124 mL.µm.m<sup>-2</sup>.24h<sup>-1</sup>.atm<sup>-1</sup>, respectively). All cross-linked fig pectin films showed 2–3 fold lower degree of swelling than CP-Ca<sup>++</sup> film. The CFP-Ca<sup>++</sup> film showed the highest surface hydrophobicity (contact angle = 101.8°) but the lowest water solubility (32.8%) and degree of swelling. Analysis of Pearson's correlations between pectin properties and film characteristics revealed that galacturonic acid (GA) content affects the mechanical properties, while GA content, degree of esterification (DE), and acetylation affect the moisture barrier performance; finally, GA content and DE affect the oxygen barrier performance of pectin films. Films of stalk waste pectins showed some properties beyond the limits of those obtained from commercial pectins.

## 1. Introduction

Sun-drying is an ancient process that has been used extensively in the Mediterranean region to obtain dried fruits. However, the quality of the final product in this process is highly variable since it is highly affected by climate and field practices. Turkey, with its 85,500 metric tons of production in the 2020/21 season, is the largest producer and exporter of sun-dried figs in the world (Anonymous, 2021). Due to the great variation in their quality, sun-dried figs are classified as extra quality, class I and class II (UNECE, 2016). A considerable part of the fruits is also substandard since they suffer from severe damage caused by insects, rotting, sun-scalding, split and torn, or excessive drying. Recently, a new and rapidly developing trend in processing high-quality sun-dried figs is that the extra quality sun-dried fruits rehydrated to intermediate

moisture levels (~35%) are portion packed. Then, they are pasteurized to obtain ready-to-eat, soft, and juicy shelf-stable fruits. The stalks of these premium fruits processed by this emerging method are cut and removed manually before processing. These fig stalks contain part of the flesh tissue that changes between 1 and 1.5% of total fruit weight depending on the experience of workers employed in stalk cutting. Thus, there is an increased industrial interest in the valorization of stalk wastes in the production of value-added products.

Due to their rich soluble dietary fiber content formed mainly by pectin, fig fruits are historically used as a natural laxative and have been considered as a functional food having positive health benefits on gastrointestinal disorders (Rtibi et al., 2018; Simmons & Preedy, 2016). Therefore, extraction and characterization of pectin from processing wastes of fresh or sun-dried figs have recently attracted considerable

\* Corresponding author.

E-mail address: [ahmetyemenicioğlu@iyte.edu.tr](mailto:ahmetyemenicioğlu@iyte.edu.tr) (A. Yemenicioğlu).

<https://doi.org/10.1016/j.foodhyd.2022.108136>

Received 12 May 2022; Received in revised form 7 September 2022; Accepted 8 September 2022

Available online 17 September 2022

0268-005X/© 2022 Elsevier Ltd. All rights reserved.

interest from different researchers. For example, Gharibzadeh et al. (2019a, 2019b) extracted and characterized the molecular and functional properties of pectin from peels of fresh figs. Çavdaroğlu et al. (2020) extracted pectin from whole sun-dried figs and characterized the antimicrobial properties of its emulsion-based edible films with essential oil component eugenol. Moreover, Çavdaroğlu and Yemencioğlu (2022) also characterized the molecular and functional properties of fig pectins extracted from whole substandard fruits and stalk wastes of sun-dried figs. Pectin extracted primarily from citrus peels and apple pomace is an indispensable ingredient for the food, biomedical, drug, cosmetics, and nutraceuticals industries, not only due to its techno-functional properties but also owing to health-promoting effects as soluble fiber (Gilani et al., 2008; Muñoz-Almagro, Montilla, & Villamiel, 2021a; Noreen et al., 2017; Rezvanain et al., 2017; Yang et al., 2015). The molecular architecture and functional properties of pectin from different sources are unique. Thus, studies for extraction of alternative pectins from different fruits and their agro-industrial wastes (e.g., from pomelo, berries, hawthorn, sunflower heads, pomegranate peel, cocoa husk, sugar beet pulp, tomato, carrot pomace, pumpkin waste, passion and banana fruit peels, and watermelon rind, etc.) and characterization of their functional properties have become a popular research topic (Dranca & Oroian, 2018; Gamonpilas et al., 2021; Henao-Díaz et al., 2021; Li et al., 2021; Marić et al., 2018; Muñoz-Almagro, Ruiz-Torralba, et al., 2021b; Reichembach & Petkovicz, 2021).

The edible films from pectin have been attracting increasing interest since this hydrocolloid might be used to produce different types of edible packaging such as solution-cast or compression molded self-standing films (Oliveira et al., 2021), extruded casings (Liu et al., 2007) or edible coatings (Çavdaroğlu et al., 2020). Commercial citrus and apple pectins as well as pectin from alternative sources (e.g., coffee, mango peel, passion fruit peel, hawthorn pectins, pineapple peel, lime peel, red pomelo peel) have been recently used in the development of edible packaging materials (Chamyuang et al., 2021; Henao-Díaz et al., 2021; Lozano-Grande et al., 2016; Nisar et al., 2018; Ribeiro et al., 2021; Rodsamran & Sothornvit, 2019a, 2019b; Sood & Saini, 2022). Moreover, different studies have also been performed to improve the poor mechanical and barrier (water vapor and oxygen permeability) properties of pectin films by using composite film making strategies employing alternative hydrocolloids (e.g., pumpkin protein extract, chitosan, hydroxypropyl methylcellulose, carboxymethylcellulose) (Dranca et al., 2021; Lalnunthari et al., 2020; Lozano-Grande et al., 2016; Rincón et al., 2021) or waxes (Lozano-Grande et al., 2016). The cross-linking is also an alternative strategy that could be used to improve the mechanical and barrier properties of pectin films. Pectin is an anionic polysaccharide that can be cross-linked with divalent cations such as calcium ( $\text{Ca}^{2+}$ ) and magnesium ( $\text{Mg}^{2+}$ ) (Li & Buschle-Diller, 2017; Moslemi, 2021). The cross-linking formed as a result of extensive junction zones among divalent ions and de-esterified carboxyl groups of pectin increases the mechanical strength of resulting hydrogels while decreasing their water solubility (Rezvanain et al., 2017). The cross-linking occurs extensively in low methoxyl pectins (degree of esterification <50%) and the formed network is generally explained by the classical “egg-box” model (Ngouémazong et al., 2012).

This study aimed to explore the characteristics of novel fig pectin edible films. For this purpose, pristine and  $\text{CaCl}_2$  cross-linked films of crude pectin from whole low-grade sun-dried figs and crude and purified pectins from stalk wastes separated during processing of high-quality sun-dried figs were evaluated for their detailed physicochemical properties such as solubility, swelling, hydrophobicity, mechanical and barrier properties, color and transparency, and morphological features. The properties of fig pectin films were also compared with those of commercial citrus and apple pectin films. The relevance of this work lies in the fact that it is the first study showing the advantages of fig pectin edible films over currently used commercial pectin films. Moreover, this is the first report that investigates the effect of pectin composition and molecular properties on the physicochemical characteristics of obtained

edible films by analyzing Pearson's correlation coefficients.

## 2. Materials and methods

### 2.1. Materials

Citrus pectin (CP, P9135, galacturonic acid  $\geq 79\%$ , methoxy content  $\geq 8\%$ ) was obtained from Sigma-Aldrich (St. Louis, MO, USA). Apple pectin (AP) was obtained from Tito (İzmir, Turkey). All other chemicals were reagent grade. The cut stalk waste (contains stalk and a piece of fruit flesh that accounts for 1–1.5% of total fruit flesh weight) of high-quality sun-dried figs (Cultivar Sarılop, UNECE class I, size number 9 and 10) separated during processing (fig stalk), and the low quality (UNECE substandard) sun-dried figs (Cultivar Sarılop) which are mainly processed into pastes were kindly supplied by KFC Gıda Tekstil Sanayi İthalat İhracat Yatırım A.Ş. (Menemen, Turkey). All samples used were fluorescence tested in the factory to ensure that they were free from mycotoxins. The samples were kept at  $-20^\circ\text{C}$  until they were used for pectin extraction.

### 2.2. Methods

#### 2.2.1. Pectin extraction

Crude pectin was extracted from low-grade substandard fruits or stalk waste at the optimal conditions reported by Çavdaroğlu et al., 2020 using a 6.0% (w/v) citric acid (CA) water solution at  $95^\circ\text{C}$  for 1 h. The pectin in the extract was precipitated with pure ethanol (pectin extract: ethanol ratio = 1:2, v/v) and collected by centrifugation ( $22,668 \times g$  for 10 min). The crude pectins (CFP and CSP) were obtained by drying the collected precipitates for 24 h at  $40^\circ\text{C}$ . The pure pectin (PSP) was obtained by suspending alcohol precipitated pectin in distilled water and stirring the resulting slurry with a glass rod for 10 min. The pectin was then again precipitated with ethanol (slurry:ethanol ratio = 1:1, w/w) and then collected by centrifugation. This procedure (washing with water and alcohol precipitation) was repeated twice. The purified pectin was dried for 24 h at  $40^\circ\text{C}$ .

#### 2.2.2. Molecular properties and composition of pectins

**2.2.2.1. Uronic acid content.** Uronic acid content was determined spectrophotometrically by the classical m-hydroxydiphenyl method at 520 nm using D-galacturonic acid as a standard, and results were expressed as galacturonic acid content (GA) (Blumenkrantz & Asboe-Hansen, 1973).

**2.2.2.2. Sugar composition.** Sugar composition (glucose, arabinose, galactose, and rhamnose) of pectins was determined spectrophotometrically using specific enzymatic kits (for glucose: GAGO20 glucose assay kit of Sigma-Aldrich, St. Louis, MO, USA; for arabinose/galactose and rhamnose: K-ARGA and K-RHAMNOSE kits of Megazyme Ltd., Ireland, respectively) as described in Çavdaroğlu and Yemencioğlu (2022). Sugar molar ratios were calculated according to Denman and Morris (2015) with the following equations:

$$R1 \text{ (mol\%, linearity of pectin)} = \frac{GA \text{ (mol\%)}}{Rha \text{ (mol\%)} + Ara \text{ (mol\%)} + Gal \text{ (mol\%)}} \quad (1)$$

$$R2 \text{ (mol\%, related with RG - I fraction content of pectin)} = \frac{Rha \text{ (mol\%)}}{GA \text{ (mol\%)}} \quad (2)$$

$$R3 \text{ (mol\%, degree of branching of RG - I)} = \frac{Ara \text{ (mol\%)} + Gal \text{ (mol\%)}}{Rha \text{ (mol\%)}} \quad (3)$$

$$R4 (\text{mol}\%, \text{ length of Gal branching in RG} - I) = \frac{\text{Gal} (\text{mol}\%)}{\text{Rha} (\text{mol}\%)} \quad (4)$$

The molar percentage of homogalacturonan (HG) and rhamnogalacturonan-I (RG-I) were calculated as according to M'sakni et al. (2006) as follows:

$$HG (\%) = GA (\text{mol}\%) - Rha (\text{mol}\%) \quad (5)$$

$$RG - I (\%) = [GA (\text{mol}\%) - HG (\%)] + Rha (\text{mol}\%) + Ara (\text{mol}\%) + Gal (\text{mol}\%) \quad (6)$$

**2.2.2.3. Degree of esterification and acetylation.** Degree of esterification (DE) of pectins was determined by the classical titrimetric method (Owens et al., 1952). The degree of acetylation (DA) of pectins was determined by minor modification of the HPLC method given by Vora-gen et al. (1986). Briefly, 30 mg of pectin was suspended in a 1 mL 0.25 M NaOH solution and held at ambient temperature for 2 h. The suspension was then centrifuged at  $10,000 \times g$  at  $4^\circ\text{C}$  for 10 min, and 20  $\mu\text{L}$  of the clear supernatant was injected into the HPLC column (Aminex HPX-87H, Biorad,  $300 \times 7.8$  mm). The column was operated at  $35^\circ\text{C}$  with a flow rate of 0.6 mL/min for 5 mM  $\text{H}_2\text{SO}_4$  used as the mobile phase. Components eluted from the column were detected with a refractive index detector which was performed in duplicate. The DA was expressed as the percent molar ratio of acetic acid to GA.

**2.2.2.4. Compositional analysis.** Moisture and ash contents were determined according to AOAC (AOAC, 1990). Soluble protein contents of pectins were determined by the Bradford method (Bradford, 1976). The phenolic content of extracted pectin was determined spectrophotometrically at 760 nm using the Folin-Ciocalteu's reagent as a reactive compound and gallic acid (GAE) as a standard (Singleton & Rossi, 1965). All analyses were performed in triplicate.

### 2.2.3. FTIR analysis

Fourier transform infrared (FTIR) spectra of pectins were obtained using a PerkinElmer FTIR spectrometer (Spectrum 100, PerkinElmer, Waltham, MA, ABD). The pectin samples were mixed with KBr at a ratio of 1:100. Spectra were collected as an average of 32 scans in the range  $4000\text{--}450$   $\text{cm}^{-1}$  with a resolution of  $4$   $\text{cm}^{-1}$  (Jafari et al., 2017). The background was taken under the same conditions with the air. The spectrum of each sample was collected three times, and their averages were taken.

### 2.2.4. Film preparation

For the preparation of films, solutions of different pectins at 3% (w/v) were heated using a hot plate working under continuous stirring at  $60^\circ\text{C}$  for 30 min. The solutions were then cooled to room temperature and further treated at 10,000 rpm for 1 min using a homogenizer-disperser (Heidolph, Germany, rotor  $\phi = 6.6$  mm Tip). Then, 0.9 g glycerol (30% w/w of pectin) was added as a plasticizer, and the mixture was stirred for 15 min. The solution was further homogenized at 10,000 rpm for 4 min using the homogenizer-disperser. To obtain solution-cast pristine films, 20 g portions of film solutions were poured into glass Petri dishes (inner diameter 10 cm) and the dishes were dried in a controlled test cabinet at  $25^\circ\text{C}$  and 50% RH for 24 h. The cross-linked films were obtained by treating dried films with 3% (w/w)  $\text{CaCl}_2$  solution and drying films again in the controlled test cabinet at  $25^\circ\text{C}$  and 50% RH for 24 h (Rezvanain et al., 2017). The pristine and cross-linked films of crude pectins from low-grade whole substandard fruits and stalk waste were designated CFP and CFP- $\text{Ca}^{++}$ , and CSP and CSP- $\text{Ca}^{++}$ , while pristine and cross-linked films of purified pectin from stalk waste were designated PSP and PSP- $\text{Ca}^{++}$ , respectively. The pristine and cross-linked commercial citrus and apple pectins films were designated CP and CP- $\text{Ca}^{++}$ , and AP and AP- $\text{Ca}^{++}$ , respectively. All pectin films

were prepared in duplicate.

### 2.2.5. Mechanical properties of films

Tensile strength at break (TS), elongation at break (EAB), and Young's modulus (YM) of films were determined using a Texture Analyzer TA-XT2 (Stable Microsystems, Godalming, UK) according to ASTM Standard Method D 882-02 (ASTM, 2002a). The dried films were conditioned in a controlled test cabinet at  $25^\circ\text{C}$  and 50% relative humidity (RH) for 24 h before testing. Then, the films were cut into 50 mm long and 8 mm wide strips. The initial grip distance was 50 mm, and the drawing speed was  $50$   $\text{mm min}^{-1}$ . Minimum eight strips of each film were tested. The thickness of films was measured by using a micrometer (Chronos, UK).

### 2.2.6. Water vapor permeability of films

The WVP of pectin films was measured using Payne permeability cups (Elcometer 5100, England) according to the ASTM Standard Method E96 (ASTM, 2016). Each cup was filled with 3 g of dried silica beads. A film (diameter: 6 cm) and an o-ring were placed on top of each cup, and cups were sealed with a metal ring with three screw clamps. The cups were weighed and then placed in a controlled test cabinet (TK 120, Nüve, Turkey) working at  $25^\circ\text{C}$  and 60% RH. The cups were weighted periodically for 72 h, and the measured weights were plotted against time. The linear portions ( $R^2 \geq 0.99$ ) of the curves with at least five data points were used for the calculation of WVP according to equation (7).

$$WVP = \frac{GL}{AtS(R_1 - R_2)} \quad (7)$$

where G is the weight change from the straight line (g), L is the thickness of the film (mm), t is the time (day), A is the test area ( $\text{m}^2$ ), S is the saturation vapor pressure at test temperature (3.169 kPa at  $25^\circ\text{C}$ ),  $R_1$  the relative humidity of the test chamber (60%) and  $R_2$  the relative humidity in the dish (0%). Four independent tests per film were performed.

### 2.2.7. Oxygen barrier properties of films

The oxygen barrier properties of the films were evaluated in terms of the oxygen transmission rate (OTR, expressed as  $\text{mL.m}^{-2}.24\text{ h}^{-1}$ ) using a Totalperm permeability analyzer (ExtraSolution® Srl, Capannori, Italy) equipped with an electrochemical sensor and based on the isostatic method, according to the standard method of ASTM F1927 at  $23^\circ\text{C}$  and 75% RH (ASTM, 1999). Specimens were mounted between two aluminum-tape masks, allowing a surface of  $2.01$   $\text{cm}^2$  to be exposed to the permeation of oxygen. All the tests were carried out with a carrier flow ( $\text{N}_2$ ) of  $35$   $\text{mL min}^{-1}$  and at 1 atm oxygen partial pressure difference on the two sides of the specimen. To reset any difference in the OTR values possibly arising from different thicknesses of the specimens, OTR values were converted to a permeability coefficient ( $P'O_2$ ) according to equation (8) (Uysal Unalan et al., 2015):

$$P'O_2 = PO_2 \times t = \frac{OTR}{\Delta p} \times t \quad (8)$$

where  $P'O_2$  is the oxygen permeability coefficient ( $\text{mL.}\mu\text{m.m}^{-2}.24\text{ h}^{-1}$   $\text{atm}^{-1}$ ),  $PO_2$  is the permeance (defined as the ratio of the OTR to the difference between the partial pressure of the vapor on the two sides of the film,  $\Delta p$ ), and t is the total thickness of the material. Each OTR value was from three replicates.

### 2.2.8. Film solubility

Before determining their solubilities, the moisture content of the films was determined by the vacuum oven method applied at  $70^\circ\text{C}$  and 16.9 kPa for 24 h. Eight pieces of each film were measured for their moisture contents. The solubility of films was determined according to the method described by Pérez et al. (2016). Briefly, pieces of films (15

× 7.5 mm<sup>2</sup>) were placed into a test tube with 10 mL of distilled water. The tubes were then shaken at 240 rpm for 24 h using an orbital shaker (IKA, OS 5 basic, Germany) and placed in an incubator at 25 °C and 50% RH. After that, the remaining solids in the tubes were collected by filtration. The insoluble dry matter content was determined by hot air drying at 105 °C until reaching constant weight. Eight pieces from each film were tested for their solubility. The film solubility (%) was determined from equation (9):

$$\text{Film solubility (\%)} = 100 \times \frac{(\text{Initial dry matter} - \text{Insoluble dry matter})}{\text{Initial dry matter}} \quad (9)$$

### 2.2.9. Degree of film swelling

The degree of swelling of the films was determined by the gravimetric method. The films (30 × 10 mm<sup>2</sup>) held in distilled water at room temperature were drained and weight periodically at 7.5, 15, and 30 min. The degree of swelling (SW) was determined using equation (10):

$$SW = 100 \times \left( \frac{W_w - W_d}{W_d} \right) \quad (10)$$

where  $W_d$  is the weight of dried film;  $W_w$  is the weight of the swelled film. Three pieces from each film were tested for their swelling degree.

### 2.2.10. Wettability of films

Wettability of pectin films was assessed by water contact angle measurements which were performed using an optical contact angle apparatus (OCA 15 Plus, Data Physics Instruments GmbH, Filderstadt, Germany) equipped with a high-resolution CCD camera and a high-performance digitizing adapter. SCA20 software (Data Physics Instruments GmbH, Filderstadt, Germany) was used for the image capturing and contact angle determination. Rectangular specimens (3 × 1.5 cm<sup>2</sup>) were kept flat throughout the analysis, and the contact angle of water in the air ( $\theta$ , °) was measured by gently dropping a droplet of 4.0 ± 0.5 mL of Milli-Q water (18.3 MV cm) onto the pectin films surface at 23 ± 1 °C and 50 ± 2% RH. The experiments were done in triplicates.

### 2.2.11. Morphological properties of films by AFM and SEM

The surface topographical images of films were obtained by atomic force microscopy (AFM, MMSPM Nanoscope 8 from Bruker, USA) in an intermittent-contact mode in the air with silicon tips (resonance frequency ≈340 kHz, spring constant ≈40 N m<sup>-1</sup>, tip radius 8 nm). The captured images (minimum 4 for each sample) were analyzed by Nanoscope Analysis software v.1.5 (Bruker, USA). The surface roughness ( $R_{rms}$ ) was calculated from Equation (11) as the root mean square average of height deviations ( $Z_i$ ) taken from a mean data plane ( $\underline{Z}$ ).

$$R_{rms} = \sqrt{\frac{\sum_{i=1}^N (Z_i - \underline{Z})^2}{N - 1}} \quad (11)$$

The  $R_{max}$  parameter indicates the maximum vertical distance between the highest and the lowest points in the image.

The surface and cross-sectional morphologies of pectin films were also examined using a scanning electron microscope (SEM, 250 Quanta FEG, FEI Company, USA). Before the experiment, the films were first freeze-dried and then placed into liquid nitrogen and crashed for the SEM examination. After that, the samples were gold-coated with a sputter coater (Emitech K550X, Quorum Technologies Inc., UK) at 10 mA for 60 s.

### 2.2.12. Transparency and color of films

Film transparency was determined according to ASTM, 2002b with modifications of the method described by Pérez et al. (2016). The transparency of films was measured at 600 nm using a spectrophotometer. Rectangular pieces of films (30 × 10 mm<sup>2</sup>) were placed into the spectrophotometer cell, and readings were taken against the empty cell used as a blank. Eight replicates of each film were tested. Transparency

was calculated from Equation (12).

$$T_{600} = \frac{(\log \%T)}{b} \quad (12)$$

where  $b$  is the film thickness (mm).

The color of films was determined using a colorimeter (CR-400, Minolta Sensing, Osaka, Japan) and recording the  $L^*$ ,  $a^*$ ,  $b^*$  values.

### 2.2.13. Statistical analysis

Statistical difference between treatments was determined by using variance analysis (one way-ANOVA) and Fisher post-hoc test ( $p \leq 0.05$ ) using Minitab (ver.18.1, Minitab Inc., United Kingdom). Pearson's correlation tests were carried out to investigate the interrelationships between the pectins' compositional or molecular properties and the film properties.

## 3. Results and discussions

### 3.1. Composition of pectins

The composition of pectins obtained from whole low-grade (sub-standard) sun-dried figs and stalk waste (composed of a stalk and adjacent fruit flesh) separated during processing of high-quality sun-dried figs were compared with those of commercial citrus and apple pectins (Table 1). The CFP showed the highest ash (~8.2%) and soluble protein (~10.4%) contents reported to be originated mainly from many tiny seeds (florets) within the fruit flesh (Çavdaroğlu et al., 2020). The high ash content determined for fig fruit pectin is also compatible with the literature that reported figs as a good source of minerals (Trad, Le Bourvellec, et al., 2014). The CSP obtained from stalk waste lacked seeds. Thus, it showed a similar composition to AP and CP. The fig stalks have no economic value and are treated currently only as waste while sub-standard figs could be utilized by alternative methods (e.g., processing into paste or ethanol and molasses depending on their quality). Moreover, Çavdaroğlu and Yemencioğlu (2022) have recently shown superior extraction yield (11.7% for stalk and 9.4% for low-grade fruits) and technological properties (e.g., better emulsion stabilizing capacity and gel textural properties) of fig stalk pectin than fig fruit pectin. Therefore, the purified pectin (PSP) in the current work was obtained using stalk wastes. The CSP and its purified form PSP contained similar ash and soluble protein contents ( $p > 0.05$ ). The soluble protein contents of CSP and PSP were found similar with CP, but significantly higher (1.7 and 1.9 fold) than that of AP. The sun-dried Sarılop figs used in the current study are also known as a good source of polyphenols (Kelebek et al., 2018). The polyphenols form a complex with polysaccharides like pectin through hydrophobic interactions (Liu et al., 2020; Tang et al., 2003). After that, the complex is stabilized with hydrogen bonds formed mainly between hydroxyl groups of polyphenols and oxygen atoms in different groups/linkages of polysaccharides (e.g., carboxyl/carboxylic acid and hydroxyl groups, the oxygen atom of glycosidic linkages) (Jakobek, 2015; Liu et al., 2020; Wu et al., 2009). In the current study, the highest total phenolic content (TPC) was determined for PSP (1.82 g GAE/100g), followed in descending order by CFP, CSP, CP, and AP. However, it should be noted that the TPCs of fig pectins in the current work were significantly lower than the TPC of ~3.0 g GAE/100 g determined for pectin extracted from peels of fresh figs (Gharibzahedi et al., 2019b).

### 3.2. Molecular properties of pectins

The GA of pectins varied between 32.2 and 80.4%. The CP showed the highest GA (80.4%) while AP (63.2%) and PSP (63%) had intermediate GAs, and crude pectins, CSP (34.2%), and CFP (32.2%) had the lowest GAs. It is important to note that the GAs determined for crude pectins extracted from sun-dried figs and their stalks were in the range of

**Table 1**

Different characteristics of fig fruit and stalk waste pectins and commercial pectins.

Characteristics <sup>a</sup>	CP <sup>b,c</sup>	AP <sup>b,c</sup>	CFP <sup>b,c</sup>	CSP <sup>b,c</sup>	PSP <sup>b,c</sup>
<b>Compositions of different pectins</b>					
<b>Moisture content</b>	12.77 ± 0.17 <sup>A</sup>	7.76 ± 0.88 <sup>C</sup>	9.10 ± 0.29 <sup>B</sup>	6.76 ± 0.11 <sup>D</sup>	5.06 ± 0.25 <sup>E</sup>
<b>Ash</b>	4.19 ± 0.20 <sup>B</sup>	4.92 ± 0.62 <sup>B</sup>	8.19 ± 0.01 <sup>A</sup>	4.61 ± 0.91 <sup>B</sup>	4.85 ± 0.37 <sup>B</sup>
<b>Soluble protein</b>	5.69 ± 1.04 <sup>B</sup>	2.96 ± 0.21 <sup>C</sup>	10.4 ± 0.31 <sup>A</sup>	4.94 ± 0.09 <sup>B</sup>	5.70 ± 0.26 <sup>B</sup>
<b>TPC<sup>d</sup></b>	0.68 ± 0.07 <sup>C</sup>	0.26 ± 0.03 <sup>D</sup>	1.25 ± 0.08 <sup>B</sup>	1.09 ± 0.05 <sup>B</sup>	1.82 ± 0.42 <sup>A</sup>
<b>Molecular properties of different pectins</b>					
<b>GA</b>	80.4 ± 7.90 <sup>A</sup>	63.2 ± 0.30 <sup>B</sup>	32.2 ± 3.94 <sup>C</sup>	34.2 ± 3.73 <sup>C</sup>	63.0 ± 4.52 <sup>B</sup>
<b>DE</b>	54.6 ± 1.46 <sup>C</sup>	60.9 ± 2.05 <sup>B</sup>	36.7 ± 3.95 <sup>E</sup>	45.0 ± 2.52 <sup>D</sup>	65.9 ± 1.89 <sup>A</sup>
<b>DA</b>	3.16 ± 0.47 <sup>D</sup>	2.22 ± 0.08 <sup>E</sup>	6.95 ± 0.83 <sup>C</sup>	11.6 ± 0.02 <sup>B</sup>	29.9 ± 3.82 <sup>A</sup>
<b>D-Glc</b>	0.24 ± 0.06 <sup>D</sup>	7.05 ± 0.23 <sup>A</sup>	5.80 ± 0.02 <sup>B</sup>	6.15 ± 0.52 <sup>B</sup>	1.72 ± 0.09 <sup>C</sup>
<b>L-Rha</b>	0.33 ± 0.09 <sup>B</sup>	1.56 ± 0.01 <sup>A</sup>	0.46 ± 0.05 <sup>B</sup>	1.81 ± 0.17 <sup>A</sup>	1.66 ± 0.40 <sup>A</sup>
<b>D-Gal</b>	3.79 ± 0.42 <sup>BC</sup>	1.53 ± 0.02 <sup>C</sup>	4.08 ± 0.19 <sup>B</sup>	3.60 ± 0.32 <sup>B</sup>	6.26 ± 0.73 <sup>A</sup>
<b>L-Ara</b>	2.96 ± 0.80 <sup>B</sup>	1.79 ± 0.07 <sup>C</sup>	3.12 ± 0.14 <sup>B</sup>	3.59 ± 0.31 <sup>B</sup>	4.92 ± 0.43 <sup>A</sup>
<b>R1<sup>e</sup></b>	9.81	10.90	3.59	3.26	4.19
<b>R2</b>	0.005	0.029	0.017	0.063	0.031
<b>R3</b>	20.96	2.14	15.51	4.03	6.74
<b>R4</b>	10.82	0.89	8.08	1.82	3.47
<b>HG (%)</b>	89.98	80.11	66.63	62.14	76.30
<b>RG-I (%)</b>	9.72	9.98	20.14	25.00	21.38

<sup>a</sup> CP: citrus pectin; AP: apple pectin; CFP: crude pectin from low-grade sun-dried figs; CSP: crude pectin from stalk waste of processed high-quality sun-dried figs; PSP: purified pectins from stalk waste of processed high-quality sun-dried figs; GA: galacturonic acid content; DE: degree of esterification; DA: degree of acetylation; D-Glc: D-glucose; L-Rha: L-rhamnose; D-Gal: D-galactose; L-Ara: L-arabinose; R1, R2, R3, R4: sugar molar ratios.; HG: The molar percentage of homogalacturonan; RG-I: The molar percentage of rhamnogalacturonan-I.

<sup>b</sup> Values are shown as mean ± standard deviation. Values at each row indicated by different letters are significantly different ( $p \leq 0.05$ ).

<sup>c</sup> All values are expressed as % on a dry basis of pectin powder except moisture content.

<sup>d</sup> TPC = total phenolic content as g GAE/100 g.

<sup>e</sup> Values are mol%.

those (24.5–33.4%) determined by Trad, Ginies, et al. (2014) for pectic compounds extracted from different fresh Tunisian fig cultivars. In contrast, the purified stalk waste pectin, PSP, showed a 1.8 fold higher GA content than its crude form (CSP). Considering the DE values, the CP, AP and PSP could be classified as high-methoxyl pectins (HMP, DE > 50%), while CSP and CFP are low-methoxyl pectins (LMP, DE < 50%). The increased DE of PSP with purification could be attributed to the increased proportion of high methoxyl GA fractions by insolubilization of LMP fractions during repeated solubilization-alcohol precipitation cycles. The sun-dried figs contain very high pectin methyltransferase activity (Demirbükler et al., 2006); thus, a heterogeneity in DE of extracted fig pectins is expected. It is also noteworthy that the GA and DE of PSP are higher than those of fresh fig peel pectin (GA: 52.5%, DE: 39%) obtained with hot acidic extraction by Gharibzahedi et al. (2019a). The DA of pectins used in the current work also showed a great variation between 2.22% and 29.9%. The fig pectins showed significantly higher DA than commercial pectins. The PSP showed the highest DA. Thus, it appears that the purification eliminated not only LMP fractions but also pectin fractions with low DA. The DE and DA are highly effective in gelation and emulsifying properties of pectins (Broxterman et al., 2017; Schmidt et al., 2015; Vriesmann & Petkowicz, 2013). However, data about the effect of DA on film properties of pectin are scarce. In the literature, the DAs of some pectins were given as follows: 3% for citrus

and 14% for pear pectins (Voragen et al., 1986), 18–58% for okra pectins (Sengkhampan et al., 2009), 17% for cacao pod husk pectin (Vriesmann & Petkowicz, 2013), 20% for carrot pectin (Broxterman et al., 2017), and 16–46.2% for sugar beet pectin (Bindereif et al., 2021).

The sugar molar ratios (R1, R2, R3, and R4) of pectins were also estimated by determining the amount of their major sugars, D-glucose (D-Glc), L-rhamnose (L-Rha), D-galactose (D-Gal), and L-arabinose (L-Ara) (Çavdaroğlu & Yemencioğlu, 2022). The D-Glc content of CSP, CFP, and AP did not vary considerably and changed between 5.80 and 7.05%, while CP obtained from citrus peels contained a limited D-Glc content. It is also important to report that the purification caused almost 3.6 fold lower glucose content for PSP than CSP, which is the crude form of PSP. The CP and CFP showed low levels of L-Rha while AP, CSP, and PSP contained significantly higher L-Rha (3.4–5.5 fold) than these two pectins ( $p \leq 0.05$ ). The highest D-Gal content was found for PSP (6.3%), followed by slightly to moderately lower D-Gal contents of CFP, CP, and CSP, and considerably lower D-Gal content of AP (1.53%). Finally, the CP, CFP, and CSP contained similar L-Ara contents ( $p > 0.05$ ) changing between 2.96 and 3.59%, while AP and PSP contained significantly lower and higher L-Ara contents than those of other pectins, respectively ( $p \leq 0.05$ ).

In plant cell walls, the pectin is mainly formed by homogalacturonan (HG, ~65%), while rhamnogalacturonan-I (RG-I, ~20–35%) is the second dominant structural form, and rhamnogalacturonan-II (RG-II, ~10%) is the minor fraction (Alba & Kontogiorgos, 2017; Basak & Annapure, 2022; Chandrayan, 2018; Yapo, 2011). Since RG-II is a very complex minor fraction composed of many different sugars, it is not considered in the theoretical calculations (Houben et al., 2011; M'sakni et al., 2006). The R1 values suggested that the AP and CP showed the highest molecular linearity while PSP had lower-intermediate linearity, and CFP and CSP had the lowest linearity. According to R2, a ratio that is an indirect indication of RG-I content, the highest value was observed for CSP, followed in descending order by PSP, AP, CFP and CP. The R3 and R4 also suggested that the degree of branching and D-Gal branch length of RG-I for pectins in descending order were as follows: CP, CFP, PSP, CSP, and AP. The calculated HG contents showed some parallelism with GA contents of CP, AP and PSP, but some variations in parallelism were observed between HG and GA of CFP and CSP. The calculated RG-I showed that the CSP and CP are the fractions with the richest and poorest RG-I contents, respectively. This finding showed parallelism with R2 ratios, which also indicates RG-I content. Both the RG-I and R2 also indicated that PSP is the second RG-I rich fraction after CSP. However, RG-I content did not show parallelism with R2 of AP and CFP, possibly due to the large differences (almost 3 fold) between their L-Rha contents that affect R2 significantly (L-Rha (mol%)/GA (mol%)).

### 3.3. FTIR spectra of pectins

The FTIR spectra of fig pectins were compared with those of commercial citrus and apple pectins to confirm their pectin structures (see supplementary file Fig. S1). It was clearly seen that the FTIR spectra of CFP, CSP and PSP showed similarities throughout the transmittance values with CP and AP. The peak between 3600 and 2300  $\text{cm}^{-1}$  reflected the stretching vibrations of the CH bond belonging to CH, CH<sub>2</sub>, and CH<sub>3</sub> groups in these pectins (Sinitnya et al., 2002). The region between 1900 and 1550  $\text{cm}^{-1}$  is important since they involve bands affected from DE and GA content of pectins. The carbonyl bands at 1630  $\text{cm}^{-1}$  and 1745  $\text{cm}^{-1}$  belong to the free carboxyl (COO<sup>-</sup>) and ester-carbonyl (C=O) groups, respectively (Fellah et al., 2009; Gnanasambandam & Proctor, 2000; Kyomugasho et al., 2015). The CH, C–OH, and  $\alpha$ -1,4 glycosidic (C–O–C) bonds in the galacturonic acid chain of pectins were also detected at 1384, 1296 and 1198  $\text{cm}^{-1}$ , respectively. All pectins gave peaks at or closely around these bands with different intensities. It was reported that the band region between 1300 and 800  $\text{cm}^{-1}$  of the spectrum is called the fingerprint region that is specific to the material structure and difficult to interpret (Jafari et al., 2017). Therefore, it was

proved that the CFP, CSP, and PSP FTIR profiles were highly comparable with those of CP and AP.

### 3.4. Mechanical properties of pectin films

Mechanical properties of pristine and CaCl<sub>2</sub> cross-linked films obtained from fig and commercial pectins are shown in Table 2. Although the cross-linking caused a significant reduction in thickness of all films, the average thicknesses of pristine and cross-linked films of citrus and fig pectins changed at a very narrow range between 84.1 and 89.0 μm and 71.2 and 78.4 μm, respectively. In contrast, pristine and cross-linked AP films were significantly thinner than all of the other respective pectin films. The results obtained for pristine films showed that the CP and PSP films had the highest tensile strengths (TSs), while AP and CSP films showed 2.4–2.8 fold lower TSs, and CFP showed 5–5.7 fold lower TS than those of CP and PSP films. The cross-linking improved the TSs of some films significantly. For example, AP-Ca<sup>++</sup>, CP-Ca<sup>++</sup>, and CFP-Ca<sup>++</sup> films showed 1.3-, 1.6- and 1.7 fold higher TSs than their pristine AP, CP, and CFP films, respectively. In contrast, no significant differences were determined between TSs of CSP and CSP-Ca<sup>++</sup> and PSP and PSP-Ca<sup>++</sup>. It is hard to understand the exact reason for failed CaCl<sub>2</sub> cross-linking to improve TS of stalk pectin films. However, it seemed that the crude and purified stalk waste pectins lacked a block-wise distribution for deesterified carboxyl groups that were essential for the formation of a highly ordered mechanically stable egg-box structure (Fraeye et al., 2009). The CP-Ca<sup>++</sup> showed the highest TS among cross-linked films followed in descending order by TSs of PSP-Ca<sup>++</sup>, AP-Ca<sup>++</sup>, CSP-Ca<sup>++</sup>, and CFP-Ca<sup>++</sup>. The CSP, AP, and CFP gave the most flexible pristine films with elongation at break (EAB) values of 26.2, 21.9, and 15.2%, respectively. The PSP films showed limited flexibility (EAB: 8.8%), while CP gave almost no flexibility (EAB: 4.2%). The cross-linking caused a significant reduction (1.8–3.7 fold) in EAB of most pectin films, except for CP films that gave similar EAB for pristine and cross-linked films. According to Young's modulus (YM) values, the CP-Ca<sup>++</sup> and PSP-Ca<sup>++</sup> films were the stiffest films, followed in descending order by CP and PSP films showing intermediate stiffness and by AP-Ca<sup>++</sup>, CSP-Ca<sup>++</sup>, CP-Ca<sup>++</sup>, CSP, CFP, AP films showing

**Table 2**  
Mechanical properties of pectin films.

Sample	Thickness (μm)	Tensile Strength (MPa)	Elongation at break (%)	Young's modulus (MPa)
CP	87.81 ± 2.04 <sup>A</sup>	17.59 ± 2.50 <sup>B</sup>	4.18 ± 1.74 <sup>F</sup>	7.56 ± 0.87 <sup>BC</sup>
AP	71.28 ± 0.13 <sup>D</sup>	6.29 ± 0.31 <sup>E</sup>	21.92 ± 7.70 <sup>AB</sup>	0.52 ± 0.12 <sup>F</sup>
CFP	89.02 ± 11.71 <sup>A</sup>	3.11 ± 0.36 <sup>F</sup>	15.19 ± 1.23 <sup>BC</sup>	0.55 ± 0.05 <sup>F</sup>
CSP	84.11 ± 1.94 <sup>AB</sup>	6.50 ± 1.71 <sup>DE</sup>	26.17 ± 0.77 <sup>A</sup>	0.70 ± 0.12 <sup>F</sup>
PSP	85.83 ± 3.61 <sup>A</sup>	15.58 ± 1.02 <sup>B</sup>	8.83 ± 1.37 <sup>D</sup>	5.69 ± 1.18 <sup>C</sup>
CP-Ca <sup>++</sup>	74.70 ± 3.20 <sup>CD</sup>	27.66 ± 2.56 <sup>A</sup>	3.51 ± 0.53 <sup>F</sup>	11.92 ± 1.42 <sup>A</sup>
AP-Ca <sup>++</sup>	59.57 ± 7.41 <sup>E</sup>	8.40 ± 2.77 <sup>C</sup>	5.87 ± 1.00 <sup>E</sup>	2.77 ± 0.47 <sup>D</sup>
CFP-Ca <sup>++</sup>	71.22 ± 1.36 <sup>D</sup>	5.34 ± 0.06 <sup>E</sup>	7.88 ± 1.61 <sup>DE</sup>	1.54 ± 0.27 <sup>E</sup>
CSP-Ca <sup>++</sup>	71.89 ± 5.81 <sup>D</sup>	7.84 ± 1.23 <sup>CD</sup>	14.28 ± 5.51 <sup>C</sup>	1.55 ± 0.33 <sup>E</sup>
PSP-Ca <sup>++</sup>	78.37 ± 1.56 <sup>BC</sup>	19.14 ± 2.52 <sup>B</sup>	4.19 ± 1.34 <sup>F</sup>	8.72 ± 0.52 <sup>AB</sup>

\*Data are shown as mean ± standard deviation. Data at each column indicated by different letters are significantly different ( $p \leq 0.05$ ). CP: citrus pectin; AP: apple pectin; CFP: crude pectin from low-grade sun-dried figs; CSP: pectin from stalk waste of processed high-quality sun-dried figs; PSP: purified pectins from stalk waste of processed high-quality sun-dried figs; -Ca<sup>++</sup>: denoted for crosslinks for all pectins.

lower-intermediate to low stiffness. The overall results clearly showed that pristine and cross-linked films of PSP and CP showed similar mechanical properties, whereas pristine and cross-linked films of CSP and CFP showed similar or slightly different mechanical properties with AP. Moreover, it is also evident that the purification of CSP and use of obtained PSP in film making caused significant improvements in the mechanical strength of fig stalk waste pectin films.

In the literature, edible films from different pectins have also been characterized for their mechanical properties. For example, pristine films from pomegranate peel (3%, v/w), pineapple peel (3%, v/w), and lime peel (1%, v/w) pectins showed TS values of 2.42, 5.60, and 16.93 MPa, and EAB values of 6.55, 14.84 and 1.77%, respectively (Oliveira et al., 2016; Rodsamran & Sothornvit, 2019a, 2019b). These results suggested that the pristine films of pomegranate peel and pineapple peel pectins had comparable mechanical properties with pristine films of CFP and CSP pectins, respectively, while films of lime peel pectin showed comparable mechanical properties with films of PSP. Data on mechanical properties related to CaCl<sub>2</sub> cross-linked films of alternative novel pectins derived from wastes are limited. It was reported that the pectin obtained from mango peel could not form a film in the presence of CaCl<sub>2</sub> (Chaiwarit et al., 2020). In contrast, edible films obtained from pumpkin peel pectin (5%, v/w) showed a TS of 5.28 MPa and EAB of 14.37% after CaCl<sub>2</sub> cross-linking (Lalnunthari et al., 2020). Furthermore, in a study, cross-linking with 1% CaCl<sub>2</sub> increased the tensile strength of the commercial citrus pectin films by 1.6 fold while decreasing the elongation at break and water solubility by 1.4 and 1.6 fold, respectively (Hari et al., 2021). Similarly, a 70% increase in the toughness and 50% increase in the tensile strength were shown after PVA/commercial citrus pectin blended films were cross-linked with 4.0 wt% CaCl<sub>2</sub> solution (John et al., 2021).

The calculated Pearson's coefficient of correlations ( $r$ ) showed the factors (composition and molecular properties of pectins) affecting the mechanical properties of pristine and cross-linked films separately (see supplementary file Tables S1 and S2). The most significant positive correlations were determined between GA of pectins and TS ( $r = 0.802$  and  $0.847$ ) and YMs ( $r = 0.717$  and  $0.852$ ) of pristine and cross-linked films, respectively. The calculated HG content of pectins also showed moderately significant positive correlations with TS ( $r = 0.760$ ) and YM ( $r = 0.790$ ) of cross-linked films, but HG content of pectins showed less significant ( $r < 0.7$ ) correlations with TS and YM of pristine films. Moreover, a moderate positive correlation was also determined between the DE of pectins and TS of pristine films ( $r = 0.726$ ). As expected, moderately significant negative correlations also existed between GA of pectins and EAB of pristine ( $r = -0.734$ ) and cross-linked ( $r = -0.794$ ) films. These results clearly showed that the GA is the primary factor giving the mechanical strength and stiffness of both pristine and cross-linked films. The R2 of pectins also showed a moderately significant positive correlation with EAB of pristine and cross-linked films ( $r = 0.728$  and  $0.727$ ), respectively. This correlation is expected since R2 was inversely proportional to the GA content of pectins. In contrast, the calculated RG-I content of pristine films did not correlate with EAB, while a weak positive correlation existed between RG-I content and EAB or cross-linked films ( $r = 0.595$ ).

### 3.5. Water vapor barrier properties

Water vapor permeability (WVP) values of different pectin films are given in Table 3. The WVP of films showed a great variation and changed between 6.3 and 31.7 g.mm.m<sup>-2</sup>.day<sup>-1</sup>.kPa<sup>-1</sup>. The PSP-Ca<sup>++</sup> with its 2–5 fold lower WVP than those of other films showed the best moisture barrier effect. The PSP, CP-Ca<sup>++</sup>, and CFP-Ca<sup>++</sup> films showed intermediate moisture barrier effects, while CSP-Ca<sup>++</sup>, CP, and AP films showed lower-intermediate, and CFP and CSP showed low moisture barrier effects. It is important to note that the cross-linking did not cause a significant change in the WVP of films obtained from CP and AP ( $p > 0.05$ ). In contrast, CFP, CSP, and PSP films showed 1.7–2 fold higher

**Table 3**Water vapor permeability (WVP), oxygen transmission rate (OTR), and permeability coefficient ( $P'O_2$ ), and thickness values of pectin films.

Film	WVP ( $\text{g}\cdot\text{mm}\cdot\text{m}^{-2}\cdot\text{day}^{-1}\cdot\text{kPa}^{-1}$ )	OTR ( $\text{mL}\cdot\text{m}^{-2}\cdot 24\text{h}^{-1}$ )	$P'O_2$ ( $\text{mL}\cdot\mu\text{m}\cdot\text{m}^{-2}\cdot 24\text{h}^{-1}\cdot\text{atm}^{-1}$ )	Thickness ( $\mu\text{m}$ )
CP	19.12 ± 1.77 <sup>BC</sup>	138.16 ± 11.8 <sup>E</sup>	10776.4 ± 922.8 <sup>E</sup>	78.2 ± 3.4 <sup>CDE</sup>
AP	21.43 ± 6.34 <sup>B</sup>	204.5 ± 9.6 <sup>C</sup>	15460.2 ± 725.8 <sup>C</sup>	75.6 ± 3.5 <sup>DE</sup>
CFP	30.39 ± 5.39 <sup>A</sup>	427.1 ± 25.2 <sup>A</sup>	51153.6 ± 3016.4 <sup>A</sup>	119.7 ± 26.1 <sup>A</sup>
CSP	31.74 ± 1.42 <sup>A</sup>	263.6 ± 19.7 <sup>B</sup>	27843.5 ± 2080.3 <sup>B</sup>	105.6 ± 4.7 <sup>AB</sup>
PSP	12.85 ± 1.24 <sup>D</sup>	173.44 ± 18.9 <sup>D</sup>	15783.04 ± 201.6 <sup>C</sup>	91 ± 4.5 <sup>BC</sup>
CP-Ca <sup>++</sup>	14.96 ± 3.38 <sup>CD</sup>	116.9 ± 6.4 <sup>E</sup>	8264.8 ± 452.5 <sup>F</sup>	70.7 ± 2.5 <sup>DE</sup>
AP-Ca <sup>++</sup>	20.31 ± 3.46 <sup>B</sup>	181.8 ± 6.7 <sup>CD</sup>	12657.4 ± 442.9 <sup>DE</sup>	66.1 ± 2.6 <sup>E</sup>
CFP-Ca <sup>++</sup>	17.45 ± 4.55 <sup>BCD</sup>	170.60 ± 20.3 <sup>D</sup>	13648.24 ± 1854.4 <sup>CD</sup>	80.3 ± 2.87 <sup>CDE</sup>
CSP-Ca <sup>++</sup>	18.11 ± 2.84 <sup>BC</sup>	58.22 ± 6.7 <sup>F</sup>	5402.82 ± 308.3 <sup>G</sup>	92.8 ± 3.7 <sup>BC</sup>
PSP-Ca <sup>++</sup>	6.28 ± 0.57 <sup>E</sup>	134.03 ± 15.2 <sup>E</sup>	11124.16 ± 1261.9 <sup>E</sup>	83 ± 3.2 <sup>CD</sup>

\*Data are shown as mean ± standard deviation. Data at each column indicated by different letters are significantly different ( $p \leq 0.05$ ). CP: citrus pectin; AP: apple pectin; CFP: crude pectin from low-grade sun-dried figs; CSP: crude pectin from stalk waste of processed high-quality sun-dried figs; PSP: purified pectins from stalk waste of processed high-quality sun-dried figs; -Ca<sup>++</sup>: denoted for cross-links for all pectins.

WVP than their respective cross-linked films ( $p \leq 0.05$ ). These results suggested that the cross-linking caused formation of denser morphologies for fig pectin films. The WVP values reported in the literature suggested that all pristine fig pectin films developed in the current work showed greater moisture barrier effects than pristine orange and mango peel pectin films (64.7–76.56  $\text{g}\cdot\text{mm}\cdot\text{m}^{-2}\cdot\text{day}^{-1}\cdot\text{kPa}^{-1}$ ) (Spatafora Salazar et al., 2019), apple pectin film prepared with pomegranate juice (72  $\text{g}\cdot\text{mm}\cdot\text{m}^{-2}\cdot\text{day}^{-1}\cdot\text{kPa}^{-1}$ ) (Azeredo et al., 2016), and pomegranate peel pectin film (60.48  $\text{g}\cdot\text{mm}\cdot\text{m}^{-2}\cdot\text{day}^{-1}\cdot\text{kPa}^{-1}$ ) (Oliveira et al., 2016). Moreover, pristine pumpkin pectin film (22.2  $\text{g}\cdot\text{mm}\cdot\text{m}^{-2}\cdot\text{day}^{-1}\cdot\text{kPa}^{-1}$ ) (Lalnunthari et al., 2020), lime peel pectin film (16.07  $\text{g}\cdot\text{mm}\cdot\text{m}^{-2}\cdot\text{day}^{-1}\cdot\text{kPa}^{-1}$ ) (Rodsamran & Sothornvit, 2019a), and lemon waste pectin-sweet potato starch blend film (23.76  $\text{g}\cdot\text{mm}\cdot\text{m}^{-2}\cdot\text{day}^{-1}\cdot\text{kPa}^{-1}$ ) (Dash et al., 2019) showed better moisture barrier effect than pristine CFP and CSP pectin films, but lower moisture barrier effect than PSP pectin films.

The Pearson's coefficient of correlations ( $r$ ) suggested that there are significant negative correlations between WVP of pristine films and GA content ( $r = -0.762$ ) and DE ( $r = -0.905$ ) of pectins used for film making. These findings suggested that pristine films with good moisture barrier properties need the use of high GA pectins, especially with a high degree of esterification. This result supported the recent finding of Huang et al. (2021), who showed that hydrophobic methyl ester groups in pectins are crucial for the moisture barrier effect of their films. On the other hand, the WVPs of cross-linked films showed a significant negative correlation with DA ( $r = -0.886$ ) of pectins used in film making. In the literature, it was reported that the high degree of acetylation interfered with the gelation of pectins since the presence of acetyl groups caused steric hindrance for chain association (Vriesmann & Petkowicz, 2013). However, it appears that the steric hindrance caused in hydrated pectin molecules by acetyl groups worked differently in dry films. It is well known that the increased degree of acetylation causes a parallel increase in the hydrophobicity of hydrocolloids such as pectin and cellulose since this replaces hydrophilic groups/bonds with hydrophobic acetyl groups (Leroux et al., 2003; Ouarhim et al., 2019). The data in the literature about the effect of acetyl groups in pectins on the WVP of their films are scarce. However, the current work showed for the first time that acetyl groups of fig pectins with DA between 6.95 and 29.9% are highly effective on the WVP of their films when these pectins were cross-linked to form an "egg-box model" configuration. The TPC did not correlate with WVP of pristine films, but it is important to note that there was a moderately significant negative correlation between the TPC of pectins and the WVP of their cross-linked films ( $r = -0.745$ ). The hydrophobic interactions formed between aromatic rings (e.g., A and C rings of flavonoids) of polyphenols and hydrophobic methyl groups of pectin are accepted as the primary mechanism of polyphenol-pectin complexation (Liu et al., 2020; Tang et al., 2003). Thus, further studies are needed to understand the effects of possible hydrophobic interactions between polyphenols and acetyl groups of pectins on the WVP of pectin films.

### 3.6. Oxygen barrier properties

The oxygen permeability coefficients ( $P'O_2$ ) of pectin films are also reported in Table 3. The best oxygen barrier performance among pristine films was observed for CP film (10776  $\text{mL}\cdot\mu\text{m}\cdot\text{m}^{-2}\cdot 24\text{h}^{-1}\cdot\text{atm}^{-1}$ ), followed by AP and PSP films with 1.4 and 1.5 fold higher, and by CSP and CFP films with almost 2.6- and 4.7 fold higher  $P'O_2$  values than that of CP film, respectively. The cross-linking significantly reduced the  $P'O_2$  of all films ( $p \leq 0.05$ ). However, the most dramatic reductions in  $P'O_2$  values of pristine films by cross-linking occurred for those of CSP and CFP films (5.2 and 3.7 fold). The cross-linking caused limited reductions in  $P'O_2$  values of PSP, CP, and AP films (1.2–1.4 fold). These results suggested dramatic changes in molecular interactions and/or morphologies in the film matrix of pristine CSP and CFP films by cross-linking. The CSP-Ca<sup>++</sup> film with a  $P'O_2$  of 8265  $\text{mL}\cdot\mu\text{m}\cdot\text{m}^{-2}\cdot 24\text{h}^{-1}\cdot\text{atm}^{-1}$  showed the highest oxygen barrier effect among the cross-linked films, followed by CP-Ca<sup>++</sup> film with 1.5 fold higher, and PSP-Ca<sup>++</sup>, AP-Ca<sup>++</sup>, CFP-Ca<sup>++</sup> films with 2.1–2.5 fold higher  $P'O_2$  values than that of CSP-Ca<sup>++</sup> film. Interestingly, the CSP film showed almost 1.8 fold higher  $P'O_2$  than PSP film, while CSP-Ca<sup>++</sup> film showed almost 2 fold lower  $P'O_2$  than PSP-Ca<sup>++</sup> film. These results clearly showed that the films of crude and purified stalk waste pectins showed considerably different oxygen barrier mechanisms in pristine and cross-linked forms. It appears that the loss of low methoxyl pectin fractions in PSP by purification is the main reason for limited changes in  $P'O_2$  of its cross-linked film.

The Pearson's coefficient of correlations ( $r$ ) showed that there are moderate to highly significant negative correlations between  $P'O_2$  of pristine films and DE ( $r = -0.838$ ), GA ( $r = -0.850$ ) and HG ( $r = -0.728$ ) of pectins used for film making. Thus, it is clear that the oxygen barrier properties of pristine films also depend on the amount of galacturonic acid units having high degree of methylation. This finding clearly explains the lower  $P'O_2$  of pristine PSP film than pristine CSP film. There is also a significant positive correlation between the soluble protein content of pectins and the  $P'O_2$  of their pristine films ( $r = 0.810$ ). This finding indicates that the soluble proteins distributed within the pectin film matrix spoiled (defected) the desired homogalacturonan film network formed by entangled linear pectin molecules. In contrast, there were no significant correlations between investigated pectin molecular and compositional parameters and  $P'O_2$  of cross-linked films. Thus, it seemed that the oxygen gas barrier effect of cross-linked films is simply a result of formed dense morphology (increased film networking) by the formation of an egg-box structure. Further studies are needed to understand the oxygen barrier properties of cross-linked pectin films.

### 3.7. Solubility and swelling of pectin films

The solubilities of pectin films are shown in Fig. 1. The pristine films of CP, AP, and PSP showed 100% solubility, while pristine CFP and CSP films showed almost 71–72% solubility due possibly to the crude and

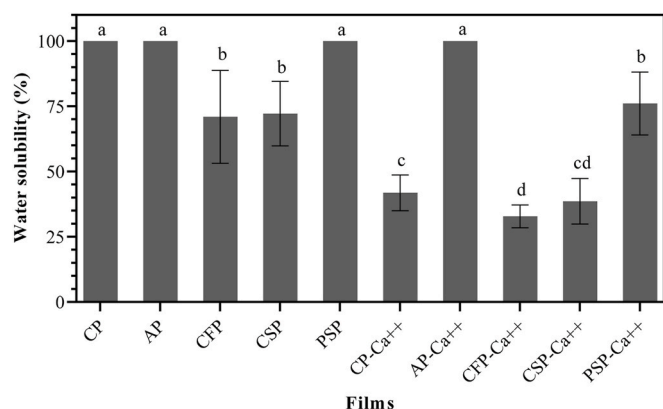


Fig. 1. Water solubility of pectin films.

heterogeneous nature of their pectins. The cross-linking caused a significant reduction in the solubility of films obtained from CP, CSP, and CFP. Thus, the lowest solubility was obtained for CFP-Ca<sup>++</sup> (32.8%) followed by CSP-Ca<sup>++</sup> (38.6%) and CP-Ca<sup>++</sup> (41.8%). This result clearly showed that the CP, CSP, and CFP pectin contained low methoxyl pectin (LMP) fractions that turned into insoluble Ca-pectate fractions. In contrast, AP-Ca<sup>++</sup> and PSP-Ca<sup>++</sup> showed 100% and 76% solubilities, respectively. The limited reduction in solubility of PSP-Ca<sup>++</sup> by cross-linking once more suggested that the purification of CSP removed mainly the LMP fractions of PSP pectin. The Pearson's coefficient of correlations ( $r$ ) suggested that there are highly significant positive correlations between water solubility of pristine films and GA ( $r = 0.851$ ), DE ( $r = 0.915$ ) and HG ( $r = 0.876$ ) of pectins. However, the only significant correlation for cross-linked films was determined between the solubility of these films and the DE of pectins ( $r = 0.783$ ) used in film making. This finding clearly showed that the DE of pectins is a very critical factor affecting the solubility of both pristine and cross-linked films.

Due to the high solubility of pristine films, the swelling properties were determined only for the cross-linked films except for that of AP-Ca<sup>++</sup> which showed 100% solubility (Fig. 2). The highest degree of swelling was observed for CP-Ca<sup>++</sup> followed in descending order by PSP-Ca<sup>++</sup>, CSP-Ca<sup>++</sup> and CFP-Ca<sup>++</sup> films that showed almost 1.9, 2.4, and 3.2 fold less swelling than CP-Ca<sup>++</sup> film, respectively. Therefore, it is clear that the CFP-Ca<sup>++</sup> films were not only the least soluble films but also the least swelling films. Due to the limited number of films used in this test, no regression analysis was conducted for film swelling.

### 3.8. Surface wettability of pectin films

The water contact angles and contact moment images of pectin films

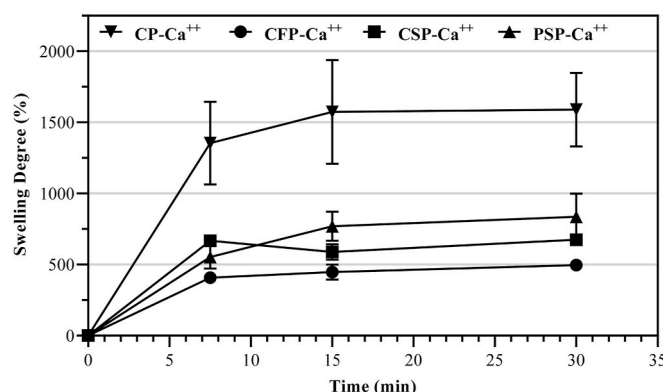


Fig. 2. Swelling curves of pectin films.

are given in Fig. 3 and Fig. 4-A to J, respectively. The film surface could act as completely wettable (hydrophilic), partially wettable, or not wettable (hydrophobic) by the solvent when the contact angle is measured at  $< 30^\circ$ , between  $30^\circ$  and  $90^\circ$ , and  $> 90^\circ$ , respectively (Chaiwarit et al., 2020). The contact angles of pristine and cross-linked pectin films varied between  $41^\circ$  and  $80^\circ$ ,  $48^\circ$  and  $102^\circ$ , respectively. None of the pectin films showed complete wettability, but the majority of films were distributed at the lower and higher limits of the partially wettable category, with the exception of CFP-Ca<sup>++</sup> that was identified as the only not wettable film under the test conditions. This result complies well with previous findings that showed the greatest resistance of CFP-Ca<sup>++</sup> films against solubility and swelling. The ranking of the hydrophobicities of pristine film surfaces in decreasing order was as follows; AP, CFP, PSP, CSP, and CP. Interestingly, the wettability values of pristine fig pectin films varied between those of two commercial pectin films. The cross-linking caused significant changes in hydrophilic/hydrophobic properties of all films ( $p > 0.05$ ). For example, CP-Ca<sup>++</sup>, CFP-Ca<sup>++</sup>, and CSP-Ca<sup>++</sup> films turned more hydrophobic (1.3 and 1.4 fold higher  $\theta$  values) than their respective pristine films (CP, CFP, CSP films) by cross-linking. This finding clearly explained the low solubility of CP-Ca<sup>++</sup>, CFP-Ca<sup>++</sup>, and CSP-Ca<sup>++</sup> films in distilled water. In contrast, AP-Ca<sup>++</sup> and PSP-Ca<sup>++</sup> films showed slightly higher hydrophilicity than their respective pristine films (AP and PSP films). Thus, the overall ranking of cross-linked film surface hydrophobicity in decreasing order was as follows; CFP-Ca<sup>++</sup>, AP-Ca<sup>++</sup>, CSP-Ca<sup>++</sup>, CP-Ca<sup>++</sup>, and PSP-Ca<sup>++</sup>.

The analysis of Pearson's coefficient of correlations suggests that there were lower-moderately significant negative correlations between water contact angle of cross-linked films and GA ( $r = -0.687$ ) content or DE ( $r = -0.686$ ) of pectins. This finding suggests that the hydrophilic groups of homopolysaccharon units have some role in determining cross-linked film surface hydrophilicity. In contrast, no significant correlations were determined between water contact angles of pristine films and molecular and compositional parameters of pectins used in film making.

### 3.9. Morphology of pectin films

The morphologies of films were investigated by AFM and SEM. The surface morphologies (Fig. 5A–J) and topographic images (Fig. 6A–J) of films obtained by AFM clearly showed that the surfaces of all pectin films were rough. The Rrms and Rmax of pectin films varied at a broad range between 7.65 and 31.9 nm and 59.9 and 224 nm, respectively (Table 4). Considering the roughness parameters, the PSP-Ca<sup>++</sup> showed the highest roughness followed in descending order by PSP and CSP films that also showed considerable roughness, and CSP-Ca<sup>++</sup>, CP-Ca<sup>++</sup>, CP, CFP films with intermediate roughness, and CFP-Ca<sup>++</sup>, AP, AP-Ca<sup>++</sup> films with limited roughness. The cross-linking caused some different

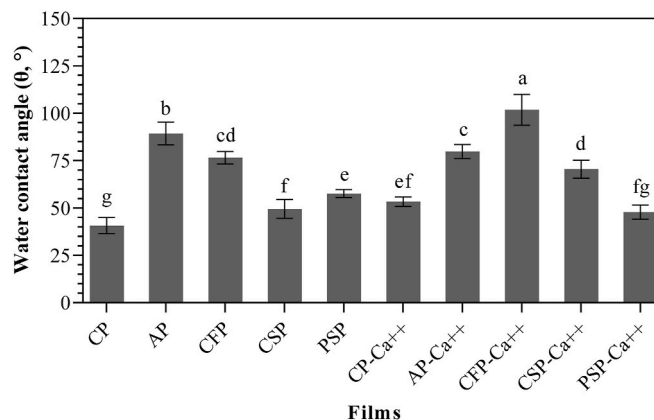


Fig. 3. Water contact angle of pectin films.

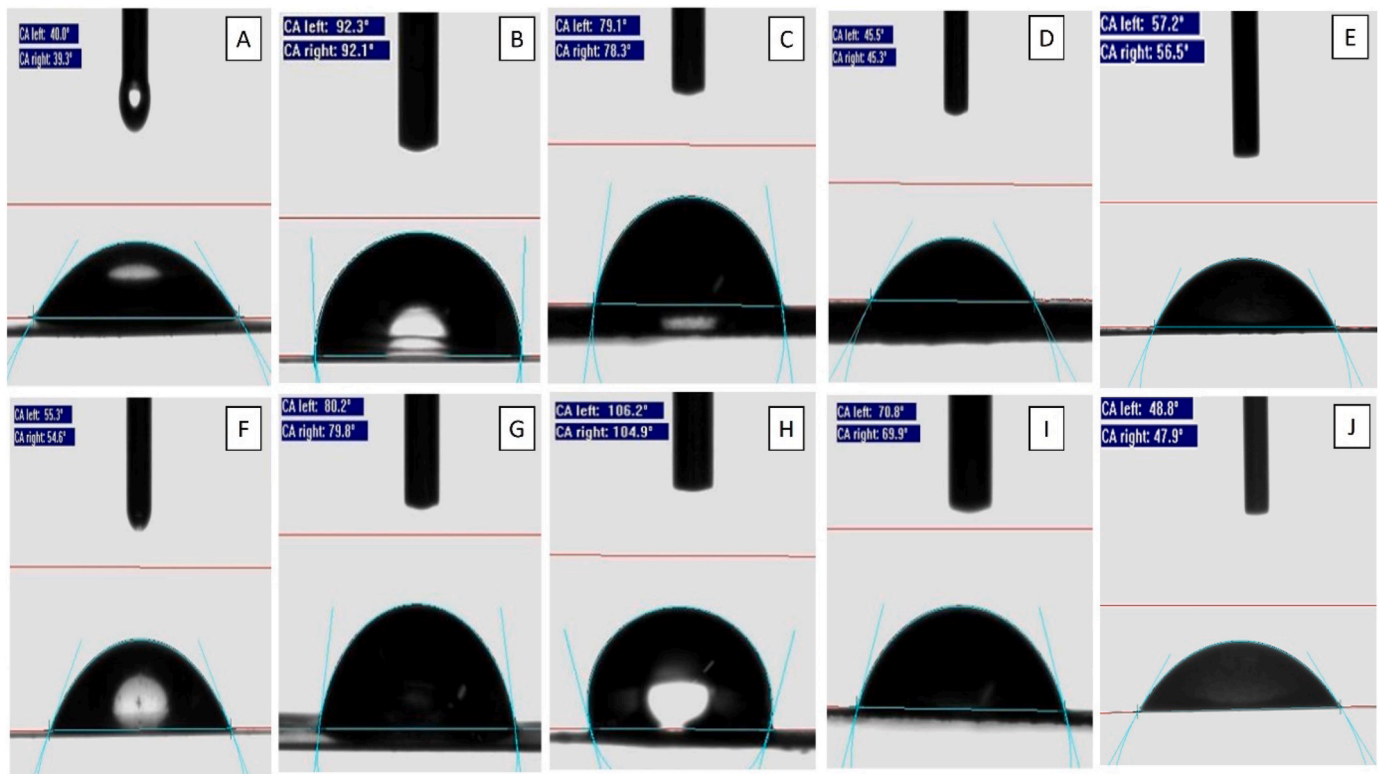


Fig. 4. Instantaneous images captured at the contact between the water droplet and the surface of pectin films: A) CP, B) AP, C) CFP, D) CSP, E) PSP, F) CP-Ca<sup>++</sup>; (G) AP-Ca<sup>++</sup>; (H) CFP-Ca<sup>++</sup>; (I) CSP-Ca<sup>++</sup>; and J) PSP-Ca<sup>++</sup>.

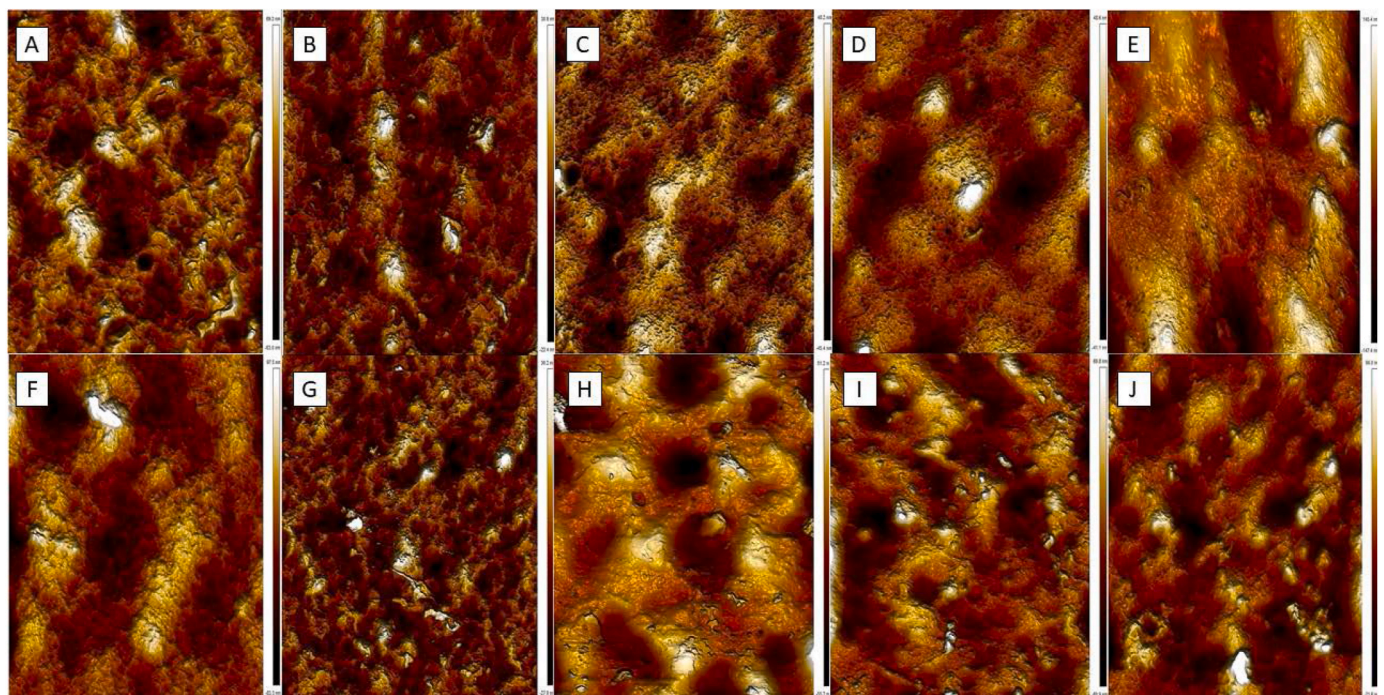


Fig. 5. Surface morphologies of pectin films: (A) CP; (B) AP; (C) CFP; (D) CSP; (E) PSP; (F) CP-Ca<sup>++</sup>; (G) AP-Ca<sup>++</sup>; (H) CFP-Ca<sup>++</sup>; (I) CSP-Ca<sup>++</sup>; and J) PSP-Ca<sup>++</sup>.

effects on the surface roughness of pectin films. For example,  $R_{rms}$  values of pristine and cross-linked films of AP, CSP, and PSP pectins were similar, while cross-linking caused a significant increase and reduction in  $R_{rms}$  values of films obtained from CP and CFP pectins, respectively. Moreover, pristine and cross-linked films of CP, AP, and

CFP pectins showed similar  $R_{max}$  values, while cross-linking caused an increase and reduction of  $R_{max}$  values for films obtained from PSP and CSP pectins, respectively. It is interesting to note that the AP films were the only ones that were not affected by cross-linking.

Fig. 7A to J shows the SEM micrographs of film surfaces at 500 ×

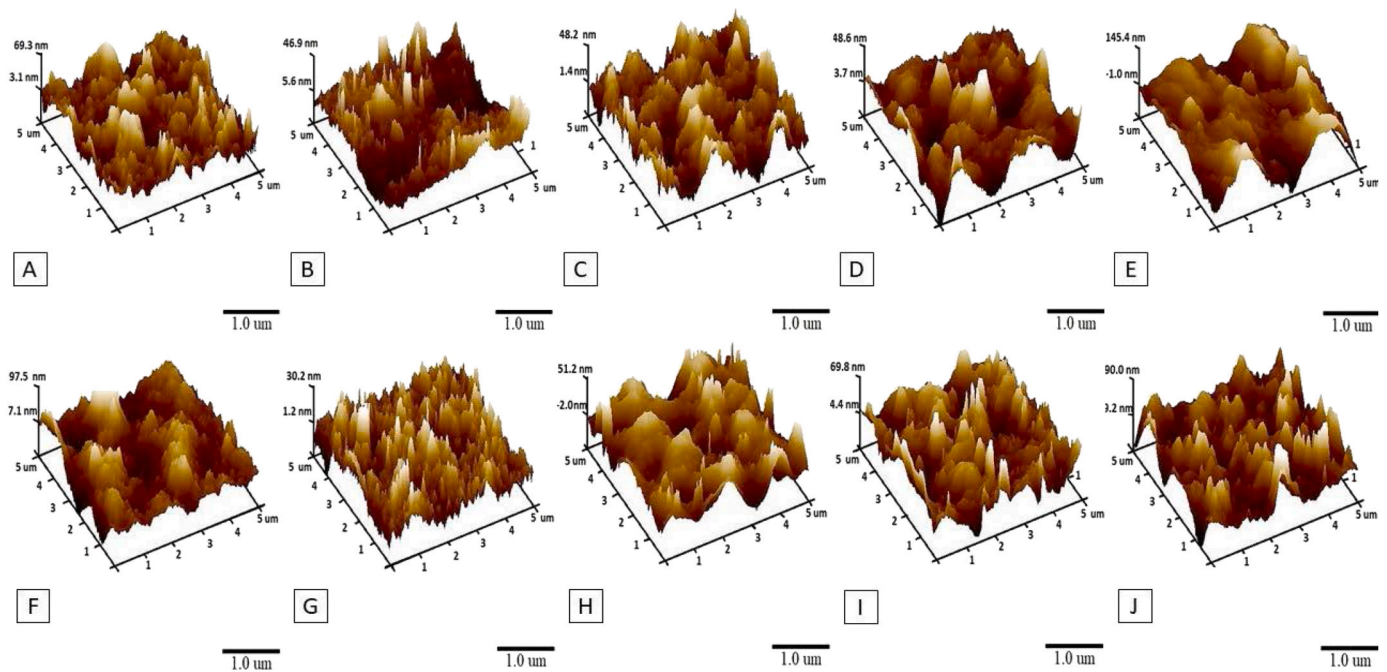


Fig. 6. Topographic images of pectin films: (A) CP; (B) AP; (C) CFP; (D) CSP; (E) PSP; (F) CP-Ca<sup>++</sup>; (G) AP-Ca<sup>++</sup>; (H) CFP-Ca<sup>++</sup>; (I) CSP-Ca<sup>++</sup>; and (J) PSP-Ca<sup>++</sup>.

Table 4

Morphological parameters of different films from AFM analysis.

Pectin film	R <sub>rms</sub> (nm) <sup>a</sup>	R <sub>max</sub> (nm)
CP	10.7 ± 1.34 <sup>D</sup>	84.0 ± 22.9 <sup>DE</sup>
AP	6.72 ± 1.81 <sup>E</sup>	68.2 ± 32.2 <sup>E</sup>
CFP	11.7 ± 2.82 <sup>CD</sup>	82.7 ± 18.1 <sup>DE</sup>
CSP	19.8 ± 6.16 <sup>B</sup>	177 ± 78.5 <sup>AB</sup>
PSP	22.8 ± 3.14 <sup>AB</sup>	157 ± 22.0 <sup>BC</sup>
CP-Ca <sup>++</sup>	16.1 ± 1.36 <sup>BC</sup>	123.9 ± 23.1 <sup>CD</sup>
AP-Ca <sup>++</sup>	7.72 ± 3.15 <sup>E</sup>	62.1 ± 13.8 <sup>E</sup>
CFP-Ca <sup>++</sup>	7.65 ± 2.18 <sup>E</sup>	59.9 ± 14.2 <sup>E</sup>
CSP-Ca <sup>++</sup>	16.4 ± 3.81 <sup>BC</sup>	118 ± 19.5 <sup>CD</sup>
PSP-Ca <sup>++</sup>	31.9 ± 5.49 <sup>A</sup>	224 ± 27.4 <sup>A</sup>

<sup>a</sup> Values at each column indicated by different letters are significantly different ( $p \leq 0.05$ ). CP: citrus pectin; AP: apple pectin; CFP: crude pectin from low-grade sun-dried figs; CSP: crude pectin from stalk waste of processed high-quality sun-dried figs; PSP: purified pectins from stalk waste of processed high-quality sun-dried figs; -Ca<sup>++</sup>: denoted for cross-links for all pectins; R<sub>rms</sub>: surface roughness; R<sub>max</sub>: maximum vertical distance.

magnification. The surfaces of pristine and cross-linked films from commercial pectins and CSP pectin were smooth and homogeneous, and they were apparently free from pores, cracks, and air bubbles. The SEM micrographs also proved that the PSP film surface was rough, but it was also evident that these films were apparently free from pores and cracks. In contrast, extensive tiny craters were clearly identifiable on both pristine and cross-linked CFP film surfaces (Fig. 7C and H). The cross-linking improved the surface smoothness of films obtained from commercial pectins and CSP pectin, but no apparent changes were observed in the surface morphologies of CFP and PSP films by cross-linking. Fig. 8A to J also shows the cross-sectional SEM images of different pectin films at 2500 × magnification (see also cross-section images during thickness measurements in supplementary file Fig. S2). The comparison of cross-sectional images of pristine and cross-linked films indicated that the cross-linking caused formation of extensive networking (intensive tiny aggregations) within films. Some heterogeneous formations were observed in CFP-Ca<sup>++</sup>, CSP-Ca<sup>++</sup> and PSP-Ca<sup>++</sup>, but CP-Ca<sup>++</sup> and AP-Ca<sup>++</sup> showed more homogeneous cross-sectional images. No apparent pores and cracks were identified at film cross-

sections, except those of CFP and CFP-Ca<sup>++</sup> films that contained some burst spherical void capsules concentrated mainly at the upper part of the film surface. The CFP pectin showed the highest soluble protein content; thus, these spherical formations might be formed by protein stabilized tiny air bubbles. These results showed that the morphology of all films changed to some extent by cross-linking. Thus, it appears that the changes in surface roughness and internal morphology together with molecular and compositional parameters determined the final mechanical and barrier properties of cross-linked pectin films. This finding also suggests that some properties of cross-linked films that lack to show any correlation with molecular and compositional parameters of pectins are affected mainly by morphological changes induced by egg-box model formation. For example, the P'O<sub>2</sub> of cross-linked films that lacked to show any correlations with parameters measured for pectin might be related mainly to changes in film morphology. Further studies are needed to determine the exact contribution of morphology to mechanical and barrier properties of pectin films.

### 3.10. Transparency and color of pectin films

The transparency values (%) of pristine films ranged between 13.8 and 27.2% (Table 5). The AP gave the most transparent pristine film followed by pristine films of CP and CSP with intermediate transparency and pristine films of PSP and CFP with low transparency. In all pristine films, the cross-linking caused a significant increase in film transparency ( $p \leq 0.05$ ). The transparency of cross-linked films ranged between 15.8 and 32.6%, but the transparency ranking for the cross-linked films is similar to that of pristine films. According to Hong et al. (2005), the transparency values of polypropylene and low-density polyethylene (LDPE) films were almost 38% and 15–20%, respectively. Thus, it appears that the transparencies of pectin films are comparable to those of LDPE films. It is important to note that CSP and CSP-Ca<sup>++</sup> films showed significantly greater transparency values than PSP and PSP-Ca<sup>++</sup> films. This finding clearly showed that the purification of fig stalk waste pectin did not result in increased film transparency. In general, film transparency is determined by morphology rather than chemical composition (Farris et al., 2009). Thus, it seemed that the difference between the transparency of crude and purified stalk waste pectin films originated from significant differences between their surface (R<sub>rms</sub> or R<sub>max</sub>) and

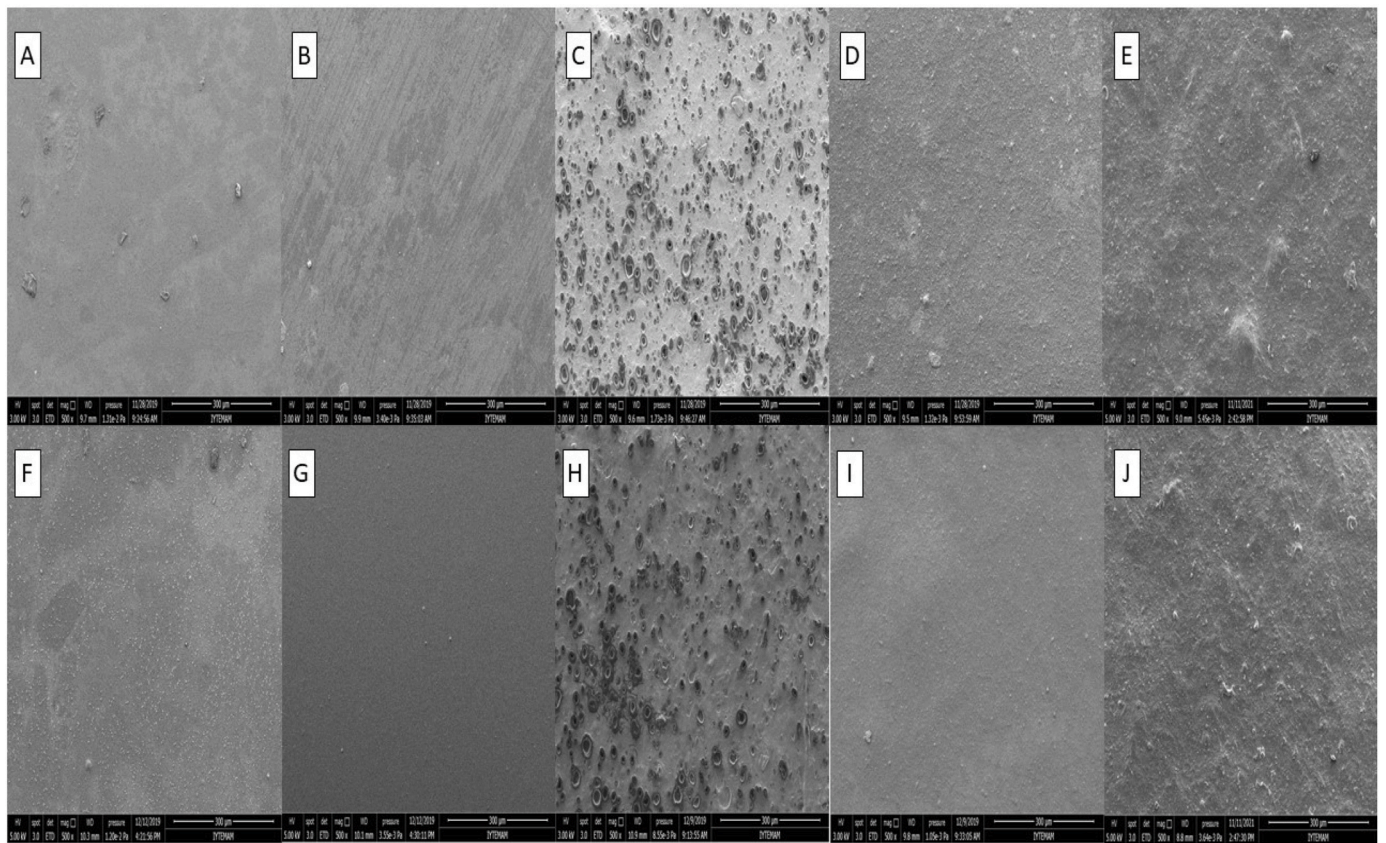


Fig. 7. Surface morphology of pectin films: (A) CP; (B) AP; (C) CFP; (D) CSP; (E) PSP; (F) CP-Ca<sup>++</sup>; (G) AP-Ca<sup>++</sup>; (H) CFP-Ca<sup>++</sup>; (I) CSP-Ca<sup>++</sup>; and (J) PSP-Ca<sup>++</sup>. (Magnification: 500 × , Scale bar: 300 µm).

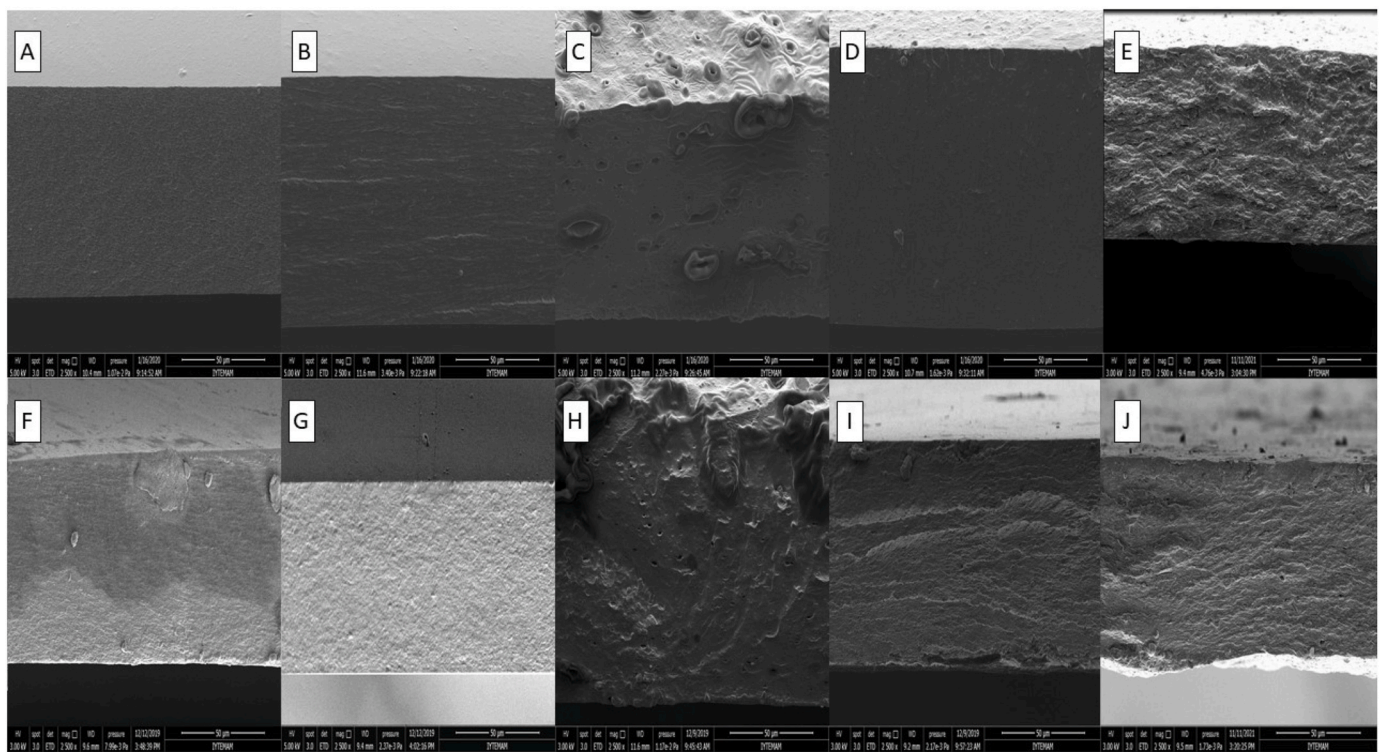


Fig. 8. Cross-sectional morphology of pectin films: (A) CP; (B) AP; (C) CFP; (D) CSP; (E) PSP; (F) CP-Ca<sup>++</sup>; (G) AP-Ca<sup>++</sup>; (H) CFP-Ca<sup>++</sup>; (I) CSP-Ca<sup>++</sup>; and (J) PSP-Ca<sup>++</sup>. (Magnification: 2500 × , Scale bar: 50 µm).

**Table 5**  
Transparency and color values of pectin films.

Sample	Transparency	L <sup>a</sup>	a <sup>a</sup>	b <sup>a</sup>
CP	21.40 ± 0.17 <sup>E</sup>	77.27 ± 1.32 <sup>C</sup>	-2.68 ± 0.61 <sup>E</sup>	34.85 ± 2.64 <sup>C</sup>
AP	27.22 ± 0.02 <sup>B</sup>	85.84 ± 0.83 <sup>A</sup>	-2.96 ± 0.06 <sup>E</sup>	11.6 ± 1.76 <sup>F</sup>
CFP	13.76 ± 0.30 <sup>I</sup>	77.77 ± 0.32 <sup>F</sup>	4.05 ± 0.21 <sup>C</sup>	42.18 ± 0.33 <sup>A</sup>
CSP	20.01 ± 0.23 <sup>F</sup>	68.66 ± 0.11 <sup>E</sup>	2.00 ± 0.09 <sup>D</sup>	37.12 ± 0.37 <sup>BC</sup>
PSP	13.77 ± 0.85 <sup>I</sup>	71.78 ± 0.71 <sup>D</sup>	5.15 ± 0.28 <sup>B</sup>	30.78 ± 0.79 <sup>D</sup>
CP-Ca <sup>++</sup>	24.83 ± 0.11 <sup>C</sup>	79.36 ± 1.03 <sup>B</sup>	1.58 ± 0.26 <sup>D</sup>	25.35 ± 2.11 <sup>E</sup>
AP-Ca <sup>++</sup>	32.59 ± 0.01 <sup>A</sup>	85.65 ± 0.2 <sup>A</sup>	1.76 ± 0.07 <sup>D</sup>	8.02 ± 0.58 <sup>G</sup>
CFP-Ca <sup>++</sup>	17.34 ± 1.43 <sup>G</sup>	66.33 ± 2.79 <sup>F</sup>	8.48 ± 1.74 <sup>A</sup>	38.65 ± 2.83 <sup>B</sup>
CSP-Ca <sup>++</sup>	23.44 ± 0.09 <sup>D</sup>	70.49 ± 0.44 <sup>DE</sup>	5.73 ± 0.15 <sup>B</sup>	31.96 ± 0.61 <sup>D</sup>
PSP-Ca <sup>++</sup>	15.79 ± 0.82 <sup>H</sup>	71.25 ± 0.66 <sup>D</sup>	5.42 ± 0.29 <sup>B</sup>	31.27 ± 0.77 <sup>D</sup>

<sup>a</sup> Data are shown as mean ± standard deviation. Data at each column indicated by different letters are significantly different ( $p \leq 0.05$ ). CP: citrus pectin; AP: apple pectin; CFP: crude pectin from low-grade sun-dried figs; CSP: crude pectin from stalk waste of processed high-quality sun-dried figs; PSP: purified pectins from stalk waste of processed high-quality sun-dried figs; -Ca<sup>++</sup>: denoted for cross-links for all pectins; L\*: lightness; a\*:redness; b\*: yellowness.

cross-sectional morphologies.

The color of films evaluated considering lightness (L\*), yellowness (a\*), and redness (b\*) values and photos of films were given in Table 5 and Fig. 9, respectively. The L\* values of films changed between 66.3 and 85.8. The cross-linking did not cause a considerable change in the L\* value of films except CP which showed a slight increase in L\* by cross-linking. The AP and CP gave the lightest colored films (Fig. 9A–D), while all fig pectin films were dark-colored (Fig. 9E–J) due to the Maillard reaction products that formed a tight complex with the extracted pectins. However, it must be noted that the purified PSP contained less Maillard reaction products, thus, it gave lighter films than CSP that is a

crude stalk waste pectin. The pristine fig pectin films also showed significantly higher a\* values than pristine commercial pectin films ( $p \leq 0.05$ ). The cross-linking increased the a\* values of films except for pristine PSP films that showed similar a\* with PSP-Ca<sup>++</sup> films. The b\* values of fig pectin films were comparable with those of CP films, while AP showed considerably lower b\* values than all pectin films.

#### 4. Conclusions

This work clearly showed the potential advantages of using pectins extracted from stalk waste of processed high-quality figs in the development of edible films. Edible films of purified stalk waste pectin showed superior mechanical strength than commercial apple pectin, while having comparable mechanical strength with commercial citrus pectin. The pristine and cross-linked films of purified stalk waste pectin had the highest moisture barrier effects, while cross-linked crude stalk waste pectin film showed the highest oxygen gas barrier effect. The films of pectin extracted from low-grade substandard fig fruits did not show outstanding mechanical and barrier properties, but the cross-linked films of this pectin showed the highest surface hydrophobicity, and lowest solubility and swelling. The analysis of Pearson's coefficient of correlations revealed fundamental knowledge about the effects of molecular and compositional parameters of studied pectins on the properties of their pristine and CaCl<sub>2</sub> cross-linked films. The major findings are as follows: (1) galacturonic acid content of pectins is the primary factor correlating positively with mechanical strength and stiffness of pristine and cross-linked films, (2) moisture barrier effect of pristine films correlates with high galacturonic acid content and high degree of esterification while moisture barrier effect of cross-linked films correlates with high degree of acetylation, (3) oxygen barrier effect of pristine films correlates with the amount of galacturonic acid units having high degree of methylation, (4) the phenolic content of pectins correlates negatively with moisture barrier effect of cross-linked films while protein content of pectins correlates positively with oxygen barrier effect of pristine films.

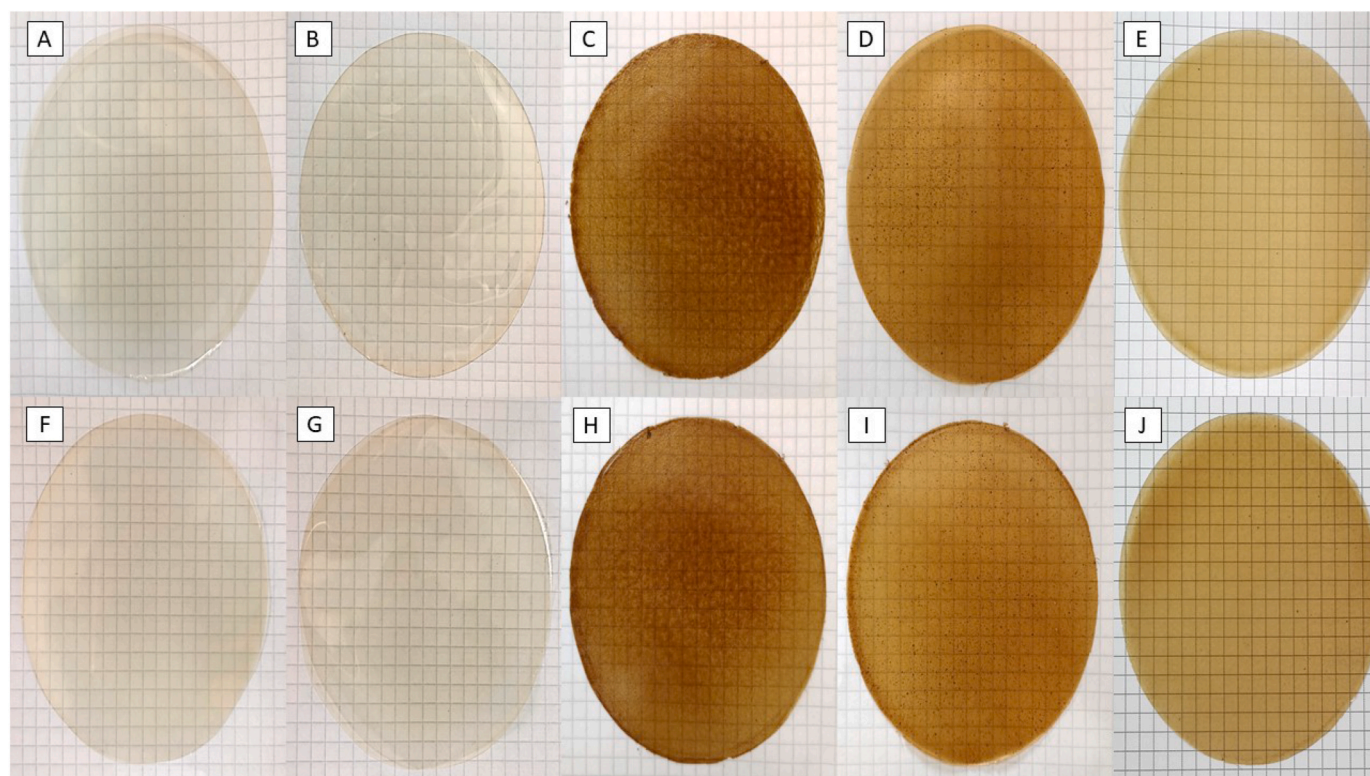


**Fig. 9.** Digital images of pectin films. Control films: A) CP, B) AP, C) CFP, D) CSP, and E) PSP; cross-linked films: F) CP-Ca<sup>++</sup>, G) AP-Ca<sup>++</sup>, H) CFP-Ca<sup>++</sup>, I) CSP-Ca<sup>++</sup>, and J) PSP-Ca<sup>++</sup>.

This work not only introduced fig stalk pectin as an alternative hydrocolloid that gives some superior edible film characteristics than commercial pectins, but also it expands the fundamental knowledge about factors affecting the mechanical and barrier properties of pectin films.

### CRedit authorship contribution statement

Elif Çavdaroğlu: Conceptualization, Investigation, Methodology, Data curation, Writing – original draft. Duygu Büyüktaş: Data curation. Stefano Farris: Conceptualization, Methodology, Writing – review & editing. Ahmet Yemenicioğlu: Conceptualization, Methodology, Supervision, Project administration, Writing – review & editing.

### Ethical guidelines

Ethics approval was not required for this research.

### Declaration of competing interest

The authors declare that they have no known competing financial interests or personal relationships that could have appeared to influence the work reported in this paper.

### Data availability

Data will be made available on request.

### Acknowledgments

This work is part of the Ph.D. thesis of author Elif Çavdaroğlu, and it was funded by The Scientific and Technological Research Council of Turkey (TÜBİTAK, Project no: 118 O 372). We thank Integrated Research Center at Izmir Institute of Technology for AFM and SEM analyses. Additionally, we thank Assoc. Prof. Dr. Ali Oğuz Büyükkileci for his guidance through the HPLC analysis. Also, we thank Prof. Dr. Banu Özen for opening FTIR in her lab and Ph.D. student Çağrı Çavdaroğlu for his assistance in FTIR analysis. Prof. Dr. Stefano Farris and Ph.D. student Duygu Büyüktaş contributed to surface wettability and OTR measurements while other experimental parts were conducted by the Ph.D. student Elif Çavdaroğlu as part of her thesis.

### Appendix A. Supplementary data

Supplementary data to this article can be found online at <https://doi.org/10.1016/j.foodhyd.2022.108136>.

### References

- Alba, K., & Kontogiorgos, V. (2017). Pectin at the oil-water interface: Relationship of molecular composition and structure to functionality. *Food Hydrocolloids*, *68*, 211–218. <https://doi.org/10.1016/j.foodhyd.2016.07.026>
- Anonymous. (2021). *Nuts and dried fruits statistical yearbook 2020/2021*. International Nut and Dried Fruit Council. Retrieved from [https://www.nutfruit.org/files/tech/1621253983\\_INC\\_Statistical\\_Yearbook\\_2020-2021.pdf](https://www.nutfruit.org/files/tech/1621253983_INC_Statistical_Yearbook_2020-2021.pdf). August 11, 2022.
- AOAC. (1990). In *Official methods of analysis* (15th ed.). Washington, DC: Association of Official Analytical Chemists.
- ASTM. (1999). *Standard test method for determination of oxygen gas transmission rate, permeability and permeance at controlled relative humidity through barrier materials a coulometric sensor*. Philadelphia, PA: American Society for Testing and Materials. *Method ASTM F 1927-98*.
- ASTM. (2002a). *Standard test method for tensile properties of thin plastic sheeting-D882-02*. In *Annual book of American standard testing methods*, *14*.
- ASTM. (2002b). *Standard test method for transparency of plastic sheeting-D 1746-97*. In *Annual book of American standard testing methods*, *8*. [https://doi.org/10.1520/C1530\\_C1530M-04R10E01](https://doi.org/10.1520/C1530_C1530M-04R10E01)
- ASTM. (2016). *Standard test methods for water vapor transmission of materials E96/E96M*. In *Annual book of ASTM standards*, *i*. [https://doi.org/10.1520/E0096\\_E0096M-16](https://doi.org/10.1520/E0096_E0096M-16)
- Azeredo, H. M. C., Morrugares-Carmona, R., Wellner, N., Cross, K., Bajka, B., & Waldron, K. W. (2016). Development of pectin films with pomegranate juice and citric acid. *Food Chemistry*, *198*, 101–106. <https://doi.org/10.1016/j.foodchem.2015.10.117>
- Basak, S., & Annappure, U. S. (2022). Trends in “green” and novel methods of pectin modification - a review. *Carbohydrate Polymers*, *278*, Article 118967. <https://doi.org/10.1016/j.carbpol.2021.118967>
- Bindereif, B., Eichhöfer, H., Bunzel, M., Karbstein, H. P., Wefers, D., & van der Schaaf, U. S. (2021). Arabinan side-chains strongly affect the emulsifying properties of acid-extracted sugar beet pectins. *Food Hydrocolloids*, *121*, Article 106968. <https://doi.org/10.1016/j.foodhyd.2021.106968>
- Blumenkrantz, N., & Asboe-Hansen, G. (1973). New method for quantitative determination of uronic acids. *Analytical Biochemistry*, *54*(2), 484–489. [https://doi.org/10.1016/0003-2697\(73\)90377-1](https://doi.org/10.1016/0003-2697(73)90377-1)
- Bradford, M. M. (1976). A dye binding assay for protein. *Analytical Biochemistry*, *72*, 248–254.
- Broxterman, S. E., Picouet, P., & Schols, H. A. (2017). Acetylated pectins in raw and heat processed carrots. *Carbohydrate Polymers*, *177*, 58–66. <https://doi.org/10.1016/j.carbpol.2017.08.118>
- Çavdaroğlu, E., Farris, S., & Yemenicioğlu, A. (2020). Development of pectin–eugenol emulsion coatings for inhibition of *Listeria* on webbed-rind melons: A comparative study with fig and citrus pectins. *International Journal of Food Science and Technology*, *55*(4), 1448–1457. <https://doi.org/10.1111/ijfs.14458>
- Çavdaroğlu, E., & Yemenicioğlu, A. (2022). Utilization of stalk waste separated during processing of sun-dried figs (*Ficus carica*) as a source of pectin: Extraction and determination of molecular and functional properties. *Lebensmittel-Wissenschaft und -Technologie*, *154*, Article 112624. <https://doi.org/10.1016/j.lwt.2021.112624>
- Chaiwarit, T., Masavang, S., Mahe, J., Sommano, S., Ruksiriwanich, W., Brachais, C.-H., Chambin, O., & Jantrawut, P. (2020). Mango (cv. Nam Dokmai) peel as a source of pectin and its potential use as a film-forming polymer. *Food Hydrocolloids*, *102*, Article 105611. <https://doi.org/10.1016/j.foodhyd.2019.105611>
- Chamyuang, S., Duangphet, S., Owatworakit, A., Intatha, U., Nacha, J., & Kerdthong, P. (2021). Preparation of pectin films from coffee Cherry and its antibacterial activity. *Trends in Sciences*, *18*(21), 34.
- Chandrayan, P. (2018). Biological function(s) and application (s) of pectin and pectin degrading enzymes. *Biosciences, Biotechnology Research Asia*, *15*(1), 87–100. <https://doi.org/10.13005/bbra/2611>
- Dash, K. K., Ali, N. A., Das, D., & Mohanta, D. (2019). Thorough evaluation of sweet potato starch and lemon-waste pectin based-edible films with nano-titania inclusions for food packaging applications. *International Journal of Biological Macromolecules*, *139*, 449–458. <https://doi.org/10.1016/j.ijbiomac.2019.07.193>
- Demirbükür, D., Simsek, S., & Yemenicioğlu, A. (2006). Potential application of hot rehydration alone or in combination with hydrogen peroxide to control pectin methylesterase activity and microbial load in cold-stored intermediate-moisture sun-dried figs. *Journal of Food Science*, *69*(3), FCT170–FCT178. <https://doi.org/10.1111/j.1365-2621.2004.tb13353.x>
- Denman, L. J., & Morris, G. A. (2015). An experimental design approach to the chemical characterisation of pectin polysaccharides extracted from *Cucumis melo inodorus*. *Carbohydrate Polymers*, *117*, 364–369. <https://doi.org/10.1016/j.carbpol.2014.09.081>
- Dranca, F., & Oroian, M. (2018). Extraction, purification and characterization of pectin from alternative sources with potential technological applications. *Food Research International*, *113*, 327–350. <https://doi.org/10.1016/j.foodres.2018.06.065>
- Dranca, F., Talón, E., Vargas, M., & Oroian, M. (2021). Microwave vs. conventional extraction of pectin from *Malus domestica* ‘Fälticeni’ pomace and its potential use in hydrocolloid-based films. *Food Hydrocolloids*, *121*, Article 107026. <https://doi.org/10.1016/j.foodhyd.2021.107026>
- Farris, S., Introzzi, L., & Piergiovanni, L. (2009). Evaluation of a bio-coating as a solution to improve barrier, friction and optical properties of plastic films. *Packaging Technology and Science*, *22*(2), 69–83. <https://doi.org/10.1002/pts.826>
- Fellah, A., Anjukandi, P., Waterland, M. R., & Williams, M. A. K. (2009). Determining the degree of methylesterification of pectin by ATR/FT-IR: Methodology optimisation and comparison with theoretical calculations. *Carbohydrate Polymers*, *78*(4), 847–853. <https://doi.org/10.1016/j.carbpol.2009.07.003>
- Fraeye, I., Dounla, E., Duvetter, T., Moldenaers, P., Van Loey, A., & Hendrickx, M. (2009). Influence of intrinsic and extrinsic factors on rheology of pectin-calcium gels. *Food Hydrocolloids*, *23*(8), 2069–2077. <https://doi.org/10.1016/j.foodhyd.2009.03.022>
- Gamonpilas, C., Buathongjan, C., Kirdsawasd, T., Rattanaprasert, M., Klomtun, M., Phonsatta, N., & Methacanon, P. (2021). Pomelo pectin and fiber: Some perspectives and applications in food industry. *Food Hydrocolloids*, *120*, Article 106981. <https://doi.org/10.1016/j.foodhyd.2021.106981>
- Gharibzadeh, S. M. T., Smith, B., & Guo, Y. (2019a). Pectin extraction from common fig skin by different methods: The physicochemical, rheological, functional, and structural evaluations. *International Journal of Biological Macromolecules*, *136*, 275–283. <https://doi.org/10.1016/j.ijbiomac.2019.06.040>
- Gharibzadeh, S. M. T., Smith, B., & Guo, Y. (2019b). Ultrasound-microwave assisted extraction of pectin from fig (*Ficus carica* L.) skin: Optimization, characterization and bioactivity. *Carbohydrate Polymers*, *222*, Article 114992. <https://doi.org/10.1016/j.carbpol.2019.114992>
- Gilani, A. H., Mehmood, M. H., Janbaz, K. H., Khan, A. ullah, & Saeed, S. A. (2008). Ethnopharmacological studies on antispasmodic and antiplatelet activities of *Ficus carica*. *Journal of Ethnopharmacology*, *119*(1), 1–5. <https://doi.org/10.1016/j.jep.2008.05.040>
- Gnanasambandam, R., & Proctor, A. (2000). Determination of pectin degree of esterification by diffuse reflectance Fourier transform infrared spectroscopy. *Food Chemistry*, *68*(3), 327–332. [https://doi.org/10.1016/S0308-8146\(99\)00191-0](https://doi.org/10.1016/S0308-8146(99)00191-0)

- Hari, K. D., Garcia, C. V., Shin, G. H., & Kim, J. T. (2021). Improvement of the UV barrier and antibacterial properties of crosslinked pectin/zinc oxide bionanocomposite films. *Polymers*, 13(15), 1–12. <https://doi.org/10.3390/polym13152403>
- Henaio-Díaz, L. S., Cadena-Casanova, C. L., Bolio López, G. L., Veleva, L., Azamar-Barrios, J. A., Hernández-Villegas, M. M., & Córdova-Sánchez, S. (2021). *Obtaining and characterization films of a bioplastic obtained from passion fruit waste (Passiflora edulis)*. *Agro Productividad*, 11. <https://doi.org/10.32854/agrop.v14i7.2010>
- Hong, S. I., Lee, J. W., & Son, S. M. (2005). Properties of polysaccharide-coated polypropylene films as affected by biopolymer and plasticizer types. *Packaging Technology and Science*, 18(1), 1–9. <https://doi.org/10.1002/pts.667>
- Houben, K., Jolie, R. P., Fraeye, I., Van Loey, A. M., & Hendrickx, M. E. (2011). Comparative study of the cell wall composition of broccoli, carrot, and tomato: Structural characterization of the extractable pectins and hemicelluloses. *Carbohydrate Research*, 346(9), 1105–1111. <https://doi.org/10.1016/j.carres.2011.04.014>
- Huang, J., Hu, Z., Hu, L., Li, G., Yao, Q., & Hu, Y. (2021). Pectin-based active packaging: A critical review on preparation, physical properties and novel application in food preservation. *Trends in Food Science & Technology*, 118(PA), 167–178. <https://doi.org/10.1016/j.tifs.2021.09.026>
- Jafari, F., Khodaiyan, F., Kiani, H., & Hosseini, S. S. (2017). Pectin from carrot pomace: Optimization of extraction and physicochemical properties. *Carbohydrate Polymers*, 157, 1315–1322. <https://doi.org/10.1016/j.carbpol.2016.11.013>
- Jakobek, L. (2015). Interactions of polyphenols with carbohydrates, lipids and proteins. *Food Chemistry*, 175, 556–567. <https://doi.org/10.1016/j.foodchem.2014.12.013>
- John, J., Deshpande, A. P., & Varughese, S. (2021). Morphology control and ionic crosslinking of pectin domains to enhance the toughness of solvent cast PVA/pectin blends. *Journal of Applied Polymer Science*, 138(18), 1–13. <https://doi.org/10.1002/app.50360>
- Kelebek, H., Dublin, S., Kadiroğlu, P., Kola, O., & Selli, S. (2018). Kurutma işlemlerinin iğnecirlerin (Ficus carica L.) fenolik bileşikleri, antioksidan kapasite ve diğer önemli bazı kalite kriterleri üzerine etkileri. *Çukurova Tarım Gıda Bil. Der.*, 33(2), 127–136.
- Kyomugasho, C., Christiaens, S., Shpigelman, A., Van Loey, A. M., & Hendrickx, M. E. (2015). FT-IR spectroscopy, a reliable method for routine analysis of the degree of methylesterification of pectin in different fruit- and vegetable-based matrices. *Food Chemistry*, 176, 82–90. <https://doi.org/10.1016/j.foodchem.2014.12.033>
- Lalnunthari, C., Devi, L. M., & Badwaik, L. S. (2020). Extraction of protein and pectin from pumpkin industry by-products and their utilization for developing edible film. *Journal of Food Science & Technology*, 57(5), 1807–1816. <https://doi.org/10.1007/s13197-019-04214-6>
- Leroux, J., Langendorff, V., Schick, G., Vaishnav, V., & Mazoyer, J. (2003). Emulsion stabilizing properties of pectin. *Food Hydrocolloids*, 17(4), 455–462. [https://doi.org/10.1016/S0268-005X\(03\)00027-4](https://doi.org/10.1016/S0268-005X(03)00027-4)
- Li, M., & Buschle-Diller, G. (2017). Pectin-blended anionic polysaccharide films for cationic contaminant sorption from water. *International Journal of Biological Macromolecules*, 101, 481–489. <https://doi.org/10.1016/j.ijbiomac.2017.03.091>
- Li, L., Gao, X., Liu, J., Chitrakar, B., Wang, B., & Wang, Y. (2021). Hawthorn pectin: Extraction, function and utilization. *Current Research in Food Science*, 4, 429–435. <https://doi.org/10.1016/j.crf.2021.06.002>
- Liu, L., Kerry, J. F., & Kerry, J. P. (2007). Application and assessment of extruded edible casings manufactured from pectin and gelatin/sodium alginate blends for use with breakfast pork sausage. *Meat Science*, 75(2), 196–202. <https://doi.org/10.1016/j.meatsci.2006.07.008>
- Liu, X., Le Bourvellec, C., & Renard, C. M. G. C. (2020). Interactions between cell wall polysaccharides and polyphenols: Effect of molecular internal structure. *Comprehensive Reviews in Food Science and Food Safety*, 19(6), 3574–3617. <https://doi.org/10.1111/1541-4337.12632>
- Lozano-Grande, M. A., Valle-Guadarrama, S., Aguirre-Mandujano, E., Lobato-Calleros, C. S. O., & Huelitl-Palacios, F. (2016). Films based on hawthorn (*Crataegus* spp.) fruit pectin and Candellilla wax emulsions: Characterization and application on pleurotus ostreatus. *Agrociencia*, 50(7), 849–866.
- Marić, M., Grassino, A. N., Zhu, Z., Barba, F. J., Brncić, M., & Rimac Brncić, S. (2018). An overview of the traditional and innovative approaches for pectin extraction from plant food wastes and by-products: Ultrasound-, microwaves-, and enzyme-assisted extraction. *Trends in Food Science & Technology*, 76, 28–37. <https://doi.org/10.1016/j.tifs.2018.03.022>
- Moslemi, M. (2021). Reviewing the recent advances in application of pectin for technical and health promotion purposes: From laboratory to market. *Carbohydrate Polymers*, 254(24), Article 117324. <https://doi.org/10.1016/j.carbpol.2020.117324>
- M'sakni, N. H., Majdoub, H., Roudesli, S., Picton, L., Le Cerf, D., Rihouey, C., & Morvan, C. (2006). Composition, structure and solution properties of polysaccharides extracted from leaves of *Mesembryanthemum crystallinum*. *European Polymer Journal*, 42(4), 786–795. <https://doi.org/10.1016/j.eurpolymj.2005.09.014>
- Muñoz-Almagro, N., Montilla, A., & Villamiel, M. (2021a). Role of pectin in the current trends towards low-glycaemic food consumption. *Food Research International*, 140, Article 109851. <https://doi.org/10.1016/j.foodres.2020.109851>
- Muñoz-Almagro, N., Ruiz-Torralba, A., Méndez-Albiñana, P., Guerra-Hernández, E., García-Villanova, B., Moreno, R., Villamiel, M., & Montilla, A. (2021b). Berry fruits as source of pectin: Conventional and non-conventional extraction techniques. *International Journal of Biological Macromolecules*, 186, 962–974. <https://doi.org/10.1016/j.ijbiomac.2021.07.016>
- Nguoumazong, D. E., Tengweh, F. F., Fraeye, I., Duvetter, T., Cardinaels, R., Van Loey, A., Moldenaers, P., & Hendrickx, M. (2012). Effect of de-methylesterification on network development and nature of Ca<sup>2+</sup>-pectin gels: Towards understanding structure-function relations of pectin. *Food Hydrocolloids*, 26(1), 89–98. <https://doi.org/10.1016/j.foodhyd.2011.04.002>
- Nisar, T., Wang, Z. C., Yang, X., Tian, Y., Iqbal, M., & Guo, Y. (2018). Characterization of citrus pectin films integrated with clove bud essential oil: Physical, thermal, barrier, antioxidant and antibacterial properties. *International Journal of Biological Macromolecules*, 106, 670–680. <https://doi.org/10.1016/j.ijbiomac.2017.08.068>
- Noreen, A., Nazli, Z. I. H., Akram, J., Rasul, I., Mansha, A., Yaqoob, N., Iqbal, R., Tabasum, S., Zuber, M., & Zia, K. M. (2017). Pectins functionalized biomaterials; a new viable approach for biomedical applications: A review. *International Journal of Biological Macromolecules*, 101, 254–272. <https://doi.org/10.1016/j.ijbiomac.2017.03.029>
- Oliveira, A. C. S., Oliveira Begali, D., Ferreira, L. F., Ugucioni, J. C., Sena Neto, A. R., Yoshida, M. I., & Borges, S. V. (2021). Effect of whey protein isolate addition on thermoplasticized pectin packaging properties. *Journal of Food Process Engineering*, 44(12). <https://doi.org/10.1111/jfpe.13910>
- Oliveira, T. Í. S., Zea-Redondo, L., Moates, G. K., Wellner, N., Cross, K., Waldron, K. W., & Azeredo, H. M. C. (2016). Pomegranate peel pectin films as affected by montmorillonite. *Food Chemistry*, 198, 107–112. <https://doi.org/10.1016/j.foodchem.2015.09.109>
- Ouarhim, W., Zari, N., Bouhfid, R., & el kacem Quais, A. (2019). Mechanical performance of natural fibers-based thermosetting composites. In M. Jawaid, M. Thariq, & N. Saba (Eds.), *Mechanical and physical testing of biocomposites, fibre-reinforced composites and hybrid composites* (pp. 43–60). Woodhead Publishing. <https://doi.org/10.1016/B978-0-08-102292-4.00003-5>
- Owens, H. S., McCreedy, R. M., Shepherd, A. D., Schultz, T. H., Phippen, E. L., Swenson, H. A., Liers, J. C., Erlandsen, R. F., & MacLay, W. D. (1952). *Methods used at western regional research laboratory for extraction and analysis of pectic materials*. Bureau of Agricultural and Industrial Chemistry.
- Pérez, L. M., Piccirilli, G. N., Delorenzi, N. J., & Verdini, R. A. (2016). Effect of different combinations of glycerol and/or trehalose on physical and structural properties of whey protein concentrate-based edible films. *Food Hydrocolloids*, 56, 352–359. <https://doi.org/10.1016/j.foodhyd.2015.12.037>
- Reichembach, L. H., & Petkowicz, C. L. de O. (2021). Pectins from alternative sources and uses beyond sweets and jellies: An overview. *Food Hydrocolloids*, 118, Article 106824. <https://doi.org/10.1016/j.foodhyd.2021.106824>
- Rezvanain, M., Ahmad, N., Mohd Amin, M. C. I., & Ng, S. F. (2017). Optimization, characterization, and in vitro assessment of alginate-pectin ionic cross-linked hydrogel film for wound dressing applications. *International Journal of Biological Macromolecules*, 97, 131–140. <https://doi.org/10.1016/j.ijbiomac.2016.12.079>
- Ribeiro, A. C. B., Cunha, A. P., da Silva, L. M. R., Mattos, A. L. A., de Brito, E. S., de Souza Filho, M. de S. M., de Azeredo, H. M. C., & Ricardo, N. M. P. S. (2021). From mango by-product to food packaging: Pectin-phenolic antioxidant films from mango peels. *International Journal of Biological Macromolecules*, 193, 1138–1150. <https://doi.org/10.1016/j.ijbiomac.2021.10.131>
- Rincón, E., Espinosa, E., García-Domínguez, M. T., Balu, A. M., Vilaplana, F., Serrano, L., & Jiménez-Quero, A. (2021). Bioactive pectic polysaccharides from bay tree pruning waste: Sequential subcritical water extraction and application in active food packaging. *Carbohydrate Polymers*, 272, Article 118477. <https://doi.org/10.1016/j.carbpol.2021.118477>
- Rodsamran, P., & Sothornvit, R. (2019a). Lime peel pectin integrated with coconut water and lime peel extract as a new bioactive film sachet to retard soybean oil oxidation. *Food Hydrocolloids*, 97, Article 105173. <https://doi.org/10.1016/j.foodhyd.2019.105173>
- Rodsamran, P., & Sothornvit, R. (2019b). Preparation and characterization of pectin fraction from pineapple peel as a natural plasticizer and material for biopolymer film. *Food and Bioproducts Processing*, 118, 198–206. <https://doi.org/10.1016/j.fbp.2019.09.010>
- Rtibi, K., Selmi, S., Grami, D., Sebai, H., & Marzouki, L. (2018). Laxative and anti-purgative bioactive compounds in prevention and treatment of functional gastrointestinal disorders, constipation and diarrhea. *Journal of Nutritional Health & Food Engineering*, 8(6), 8–10. <https://doi.org/10.15406/jnhfe.2018.08.00312>
- Schmidt, U. S., Koch, L., Rentschler, C., Kurz, T., Endreß, H. U., & Schuchmann, H. P. (2015). Effect of molecular weight reduction, acetylation and esterification on the emulsification properties of citrus pectin. *Food Biophysics*, 10(2), 217–227. <https://doi.org/10.1007/s11483-014-9380-1>
- Sengkhampan, N., Bakx, E. J., Verhoef, R., Schols, H. A., Sajjaanantakul, T., & Voragen, A. G. J. (2009). Okra pectin contains an unusual substitution of its rhamnosyl residues with acetyl and alpha-linked galactosyl groups. *Carbohydrate Research*, 344(14), 1842–1851. <https://doi.org/10.1016/j.carres.2008.11.022>
- Simmons, M. S. J., & Preedy, V. R. (2016). *Nutritional composition of fruit cultivars*. Academic Press.
- Singleton, V. L., & Rossi, J. A. J. (1965). Colorimetry of total phenolics with phosphomolibdic-phosphotungstic acid reagents. *American Journal of Enology and Viticulture*, 16, 144–158.
- Sinitnya, A., Čopíková, J., Prutyayov, V., Skoblyva, S., & Machovič, V. (2002). Amidation of highly methoxylated citrus pectin with primary amines. *Carbohydrate Polymers*, 42(4), 359–368. [https://doi.org/10.1016/S0144-8617\(99\)00184-8](https://doi.org/10.1016/S0144-8617(99)00184-8)
- Sood, A., & Saini, C. S. (2022). Red pomelo peel pectin based edible composite films: Effect of pectin incorporation on mechanical, structural, morphological and thermal properties of composite films. *Food Hydrocolloids*, 123, Article 107135. <https://doi.org/10.1016/j.foodhyd.2021.107135>
- Spatafora Salazar, A. S., Sáenz Cavazos, P. A., Mújica Paz, H., & Valdez Frago, A. (2019). External factors and nanoparticles effect on water vapor permeability of pectin-based films. *Journal of Food Engineering*, 245, 73–79. <https://doi.org/10.1016/j.jfoodeng.2018.09.002>
- Tang, H. R., Covington, A. D., & Hancock, R. A. (2003). Structure-activity relationships in the hydrophobic interactions of polyphenols with cellulose and Collagen. *Biopolymers*, 70(3), 403–413. <https://doi.org/10.1002/bip.10499>

- Trad, M., Ginies, C., Gaaliche, B., Renard, C. M. G. C., & Mars, M. (2014). Relationship between pollination and cell wall properties in common fig fruit. *Phytochemistry*, 98, 78–84. <https://doi.org/10.1016/j.phytochem.2013.12.011>
- Trad, M., Le Bourvellec, C., Gaaliche, B., Renard, C. M. G. C., & Mars, M. (2014). Nutritional compounds in figs from the southern mediterranean region. *International Journal of Food Properties*, 17(3), 491–499. <https://doi.org/10.1080/10942912.2011.642447>
- UNECE. (2016). *UNECE (united nations economic commission for europe) standard DDP-14 concerning the marketing and commercial quality control of dried figs*. Retrieved from [https://unece.org/fileadmin/DAM/trade/agr/standard/dry/dry\\_e/14DriedFigs\\_E2016.pdf](https://unece.org/fileadmin/DAM/trade/agr/standard/dry/dry_e/14DriedFigs_E2016.pdf). August 11, 2022.
- Uysal Unalan, I., Wan, C., Figiel, L., Olsson, R. T., Trabattoni, S., & Farris, S. (2015). Exceptional oxygen barrier performance of pullulan nanocomposites with ultra-low loading of graphene oxide. *Nanotechnology*, 26(27), Article 275703. <https://doi.org/10.1088/0957-4484/26/27/275703>
- Voragen, A. G. J., Schols, H. A., & Pilnik, W. (1986). Determination of the degree of methylation and acetylation of pectins by h.p.l.c. *Topics in Catalysis*, 1(1), 65–70. [https://doi.org/10.1016/S0268-005X\(86\)80008-X](https://doi.org/10.1016/S0268-005X(86)80008-X)
- Vriesmann, L. C., & Petkowicz, C. L. O. (2013). Highly acetylated pectin from cacao pod husks (*Theobroma cacao* L.) forms gel. *Food Hydrocolloids*, 33(1), 58–65. <https://doi.org/10.1016/j.foodhyd.2013.02.010>
- Wu, Y., Chen, Z., Li, X., & Li, M. (2009). Effect of tea polyphenols on the retrogradation of rice starch. *Food Research International*, 42(2), 221–225. <https://doi.org/10.1016/j.foodres.2008.11.001>
- Yang, X., Guo, J. L., Ye, J. Y., Zhang, Y. X., & Wang, W. (2015). The effects of *Ficus carica* polysaccharide on immune response and expression of some immune-related genes in grass carp, *Ctenopharyngodon idella*. *Fish & Shellfish Immunology*, 42(1), 132–137. <https://doi.org/10.1016/j.fsi.2014.10.037>
- Yapo, B. M. (2011). Rhamnogalacturonan-I: A structurally puzzling and functionally versatile polysaccharide from plant cell walls and mucilages. *Polymer Reviews*, 51(4), 391–413. <https://doi.org/10.1080/15583724.2011.615962>